

Washington University in St. Louis

Washington University Open Scholarship

Arts & Sciences Electronic Theses and
Dissertations

Arts & Sciences

Summer 8-15-2013

Various Geometric Aspects of Condensed Matter Physics

Zhenyu Zhou

Washington University in St. Louis

Follow this and additional works at: https://openscholarship.wustl.edu/art_sci_etds



Part of the [Physics Commons](#)

Recommended Citation

Zhou, Zhenyu, "Various Geometric Aspects of Condensed Matter Physics" (2013). *Arts & Sciences Electronic Theses and Dissertations*. 1049.

https://openscholarship.wustl.edu/art_sci_etds/1049

This Dissertation is brought to you for free and open access by the Arts & Sciences at Washington University Open Scholarship. It has been accepted for inclusion in Arts & Sciences Electronic Theses and Dissertations by an authorized administrator of Washington University Open Scholarship. For more information, please contact digital@wumail.wustl.edu.

WASHINGTON UNIVERSITY IN ST. LOUIS

Department of Physics

Dissertation Examination Committee:

Alexander Seidel, Chair

Mark Alford

John Clark

Renato Feres

Zohar Nussinov

Xiang Tang

Various Geometric Aspects of Condensed Matter Physics

by

Zhenyu Zhou

A dissertation presented to the
Graduate School of Arts and Sciences
of Washington University in
partial fulfillment of the
requirements for the degree
of Doctor of Philosophy

August 2013

St. Louis, Missouri

Contents

List of Figures	iv
Acknowledgements	v
Abstract	vi
1 Introduction	1
2 Heat equation approach to geometric changes of the torus Laughlin state	7
2.1 Introduction to Quantum Hall Effect	7
2.1.1 2D electron gas in a magnetic field	8
2.1.2 The integer quantum Hall effect	12
2.1.3 The fractional quantum Hall effect	14
2.1.4 Haldane's pseudopotential	18
2.2 Motivations	20
2.3 Guiding center representation of Laughlin state, from cylinder to torus	21
2.4 Construction of the 2-body operator	29
2.4.1 A final look at the cylinder case	29
2.4.2 General considerations for the generator on the torus	32
2.4.3 Heat equation for the torus Laughlin state	33
2.4.4 Mapping the problem to 1D	34
2.4.5 Definition of a 2-body operator generating the deformation of guiding center variables	36
2.4.6 Symmetry considerations	44
2.4.7 Presentation of the Laughlin state through its thin torus limit	45
2.5 Application: Hall viscosity	47
2.6 Discussion	56
3 Geometric phase of d-wave vortices in a model of lattice fermions	59
3.1 Introduction and motivation	59
3.2 Background	60
3.3 Model description	62
3.4 Calculation of the Berry phase	65
3.5 Results	67
3.6 Discussion	72

4 Summary	74
Appendices	76
.1 Analytic properties of Laughlin state coefficients	77
.2 Hilbert space reduction by magnetic translational operator	78
.3 Evaluation of second quantization of theta-function term in the generator	80
.4 Optimization of the generator in thin limit	83
Bibliography	86

List of Figures

2.1	Experimental result of integer and fractional quantum Hall effect	8
2.2	IQHE on an annulus with uniform field B. Additional solenoid is present in the center of annulus.	13
2.3	Fundamental domain for torus wave functions.	25
2.4	Commuting diagram displaying the various Hilbert spaces and sub-spaces defined in the main text, and operators acting between them.	37
2.5	Average “orbital spin per particle” \bar{s} as calculated from Eq. (2.70), for the $\nu = 1/3$ torus Laughlin state at τ generated via Eq. (2.75), using the procedure described in the main text.	54
2.6	Average orbital spin per particle \bar{s} , calculated from Eq. (2.70), for the $\nu = 1/3$ torus Laughlin state, with τ goes along unit circle.	55
3.1	A magnetic unit cell of fermionic lattice for d-wave superconductor with 2 vortices embedding. The ground state gain Berry phase when one vortex goes around a close loop.	61
3.2	Superfluid velocity in a 7 by 5 magnetic unit cell. The positions of vortices are (2,2) and (-2,-2).	64
3.3	Berry curvature for 12 by 10 lattice in the presence of two vortices, for $\mu = 0.05$. (a): 3D view of the Berry curvature in the vicinity of one plaquette. (b) Top view of the lattice. (c): 3D view of the entire lattice.	69

Acknowledgements

I will give my sincere gratitude to my advisor, Professor Alexander Seidel, for his tremendous help. His insightful understanding inspires me a lot and keeps my enthusiasm to the research from time to time. I am also benefit a lot from courses and discussions with Professor Zohar Nussinov, John Clark and Jung-Tsung Shen. I am supported by Alex through the National Science Foundation under Grant No. DMR-0907793 and National Science Foundation under NSF Grant No. DMR-1206781.

I also want to thanks to my parents and sister, for their loves and supports during all my life.

ABSTRACT OF THE DISSERTATION

Various Geometric Aspects of Condensed Matter Physics

by

Zhenyu Zhou

Doctor of Philosophy in Physics

Washington University in St. Louis, 2013

Professor Alexander Seidel, Chairperson

Geometric aspect of condensed matter has arouse a lot of interests in recent years. The idea of Berry phase is highly appreciated in various systems. We explored the geometric features of two specific electron systems, fractional quantum Hall (FQH) states and d-wave superconducting states. For FQH states, we propose a two body operator which generates the geometric change of Laughlin state in the guiding center degrees of freedom on torus. This operator therefore generates the adiabatic evolution between Laughlin states on regular tori and the quasi-one-dimensional thin torus limit. For d-wave superconducting model, we study the local and topological features of Berry phases associated with the adiabatic transport of vortices in a lattice fermions. We find bosonic statistics for vortices in hall filling. Away from half filling, we find the complicate Berry phase to be path dependent. However, it is shown that “statistical” flux attached to the vortex are still absent. The average flux density associated with Berry curvature is tied to the average density of cooper pair in the magnetic unit cell. This is familiar from dual theories of bosonic systems, even though the underlying particles are fermions in this case.

Chapter 1

Introduction

As Wheeler [73] put it, “All physics is geometry”. This notion became widely accepted since the early 20th century through Einstein’s general relativity theory. In quantum mechanics, a geometric revolution took place much later until 1950s. Through the discovery of Aharonov-Bohm (AB) [1] effect, it was realized that geometry may play a role in quantum mechanics even where it does not in classical physics. Prior to that, on the theory side, Dirac’s monopole quantization [11] can be seen as a prelude to later work by Chern on characteristic classes of vector bundles [10]. In particle physics, geometric notions gained prominence through the realization of fundamental forces as gauge forces. In the 80s, Michael Berry demonstrated that certain aspects of quantum mechanics are intrinsically geometric, even in the absence of curved space time and gauge forces [8].

Michael Berry showed that in quantum mechanical systems, an energy eigenstate picks up the “Berry phase” when it experiences an adiabatically evolution along a closed loop in some parameter space. This notion proved to be of central importance in many areas of physics. For example, fundamental phenomena already understood at the time, such as the

AB effect and Pancharatnam phase, could now be reinterpreted in the language of Berry phases. In condensed matter physics, Berry phases have useful applications in the realm of many-particle physics. They offer a route to classifying many body ground states such as quantum Hall fluids [61], Chern insulators [20], and topological insulators [17]. They are also fundamental in defining exotic statistics of the elementary excitations in some of these systems.

We will start by introducing the reader into the idea of the geometric phase and the Berry phase by some examples, both classical and quantum mechanical. A simple understanding of a geometric phase may come from the parallel transport on a sphere. A man carrying an arrow (always pointing tangentially to the surface) walks from the north pole southward to the equator. He turns and walks along the equator for some distance, then turns north back to where he began. As long as his arrow always keeps the same angle with the great circle he is walking on, he will find that the direction of the arrow is different from the beginning when he returns back to north pole. The difference is proportional to the area that his journey encloses. This is not surprising from a mathematical point of view due to the curvature of the sphere. Another famous example of a geometric phase is the Foucault pendulum, which is a common display in science museums. The vertical plane in which the pendulum is swinging will rotate with time due to the rotation of the earth. Once 24 hours, the pivot of pendulum returns to its original place in a non-rotating earth frame, but the vertical swinging plane does not go back to itself. Instead it rotates a certain angle proportional to the area that the pendulum pivot encircles in one day. This experiment was introduced early on in 1851 as a simple proof of the Earth's rotation and the explanation involves nothing more complicated than the Coriolis force. The common feature of two examples above is a

change of phase when going around a closed loop on some manifold, which is the defining feature of a geometric phase.

As mentioned, the AB effect is a common example of Berry phases in a quantum mechanical system, where a charged particle picks up an additional phase by traveling in a loop around a solenoid with non-zero magnetic flux. Classically this phase has no analog and so there is no effect, as would be expected from the fact that the field vanishes along the path of the particle. However, quantum mechanically, the wave function of the particle gains the Berry phase, which may lead to interference effects. This may be understood in a field theory language as shown in the following. The classical Lagrange function L_0 of the particle is modified by the magnetic field of the solenoid as follows ,

$$L(\mathbf{x}, \dot{\mathbf{x}}) = e\mathbf{A} \cdot \dot{\mathbf{x}} + L_0(\mathbf{x}, \dot{\mathbf{x}}) \tag{1.1}$$

Note that the vector potential \mathbf{A} does not vanish even in regions where the \mathbf{B} field is zero. However, this does not affect the classical equation of motions in such regions. In the path integral formalism, a closed path has a phase associated to it given by $\exp(\frac{i}{\hbar} \int_{t_i}^{t_f} dt L(\mathbf{x}, \dot{\mathbf{x}}))$, where \hbar is the Planck constant. The extra term in the modified Lagrange function then leads to additional phase equal to $\frac{e}{\hbar} \Phi$, where Φ is the flux through the closed path of the particle. This phase difference may lead to interference effect and to an effective change of boundary conditions if the particle is confined to a wire enclosing the solenoid. Note however, there is no effect if the additional phase is an integer multiple of 2π , or $\Phi = 2n\pi\hbar/e = nh/e$. One may notice that here appears a natural unit of flux in quantum mechanics, the so called flux quantum, $\Phi_0 = h/e$. Thus the AB phase can be written as $2\pi\Phi/\Phi_0$.

In the Hilbert space formulation of quantum mechanics, the AB phase naturally appears as a Berry phase. Here we quote the formal definition of the Berry phase as follows [8],

$$\gamma_n(C) = i \oint_C \langle n(\mathbf{R}) | \nabla_{\mathbf{R}} n(\mathbf{R}) \rangle \cdot d\mathbf{R}. \quad (1.2)$$

where C is the closed path, \mathbf{R} is the changing parameter, and $|n(\mathbf{R})\rangle$ is the energy eigenstate of the system. The berry phase γ_n is a change of phase on the state $|n\rangle$ after an adiabatically evolution around the closed path C in parameter space \mathbf{R} ,

$$|n(\mathbf{R}_f)\rangle = e^{i\gamma_n} |n(\mathbf{R}_i)\rangle, \quad (1.3)$$

where f and i refer to “final” and “initial”, although \mathbf{R}_f and \mathbf{R}_i are the same point in parameter space.

One important property of the Berry phase is gauge invariance. The integrant of Eq. 1.2 is called Berry connection, as shown below,

$$A_n(\mathbf{R}) = i \langle n(\mathbf{R}) | \nabla_{\mathbf{R}} n(\mathbf{R}) \rangle. \quad (1.4)$$

It's obvious that the Berry connection is gauge dependent. We can make a gauge transformation $|n(\mathbf{R})\rangle \rightarrow e^{i\Lambda(\mathbf{R})} |n(\mathbf{R})\rangle$, where $\Lambda(\mathbf{R})$ is arbitrary analytical function and the Berry connection transforms into $A_n(\mathbf{R}) - \nabla_{\mathbf{R}} \Lambda(\mathbf{R})$. Integration over some path adds an additional term $\Lambda(\mathbf{R}_i) - \Lambda(\mathbf{R}_f)$ to the Berry phase. However, when the path is closed, there is a single value restriction for the gauge transformation. In other words, the gauge factor $e^{i\Lambda(\mathbf{R})}$ must

be single valued. This implies, for a closed loop,

$$\Lambda(\mathbf{R}_i) - \Lambda(\mathbf{R}_f) = 2\pi \cdot \text{integer}. \quad (1.5)$$

where \mathbf{R}_i and \mathbf{R}_f correspond to the same physical point, but we allow for the multivalueness of the function Λ . Note that the integer can only be non-zero if the closed path is non-trivial geometrically. In this case Λ is called a large gauge transformation. Eq. 1.5 only changes the Berry phase by integer multiples of 2π , which has no physical effect.

The loop integral in the definition of the Berry phase can be easily transformed by Stocks's theorem into a surface integral of the so-called Berry curvature

$$\gamma_n(\partial S) = i \int_S \mathbf{B}_n(\mathbf{R}) \cdot d\mathbf{S}, \quad (1.6)$$

where the Berry curvature is $\mathbf{B}_n(\mathbf{R}) = \nabla_{\mathbf{R}} \times \mathbf{A}_n(\mathbf{R})$, which is the magnetic field in AB effect example. Berry curvature is also gauge invariant and thus observable. The integral of the Berry curvature over closed surfaces, such as sphere or torus, is a topological invariant equal to 2π times the Chern number, which leads to Dirac's magnetic monopole quantization [11] when apply to charged particle confined to a closed surface. Overall, the Berry phase is a beautiful unifying concept that has close analogies to gauge field theories and differential geometry.

The research presented in this thesis is exploring Berry phases and other geometric aspects in different condensed matter systems, specifically, fractional quantum Hall (FQH) systems and type II superconductors. This divides the thesis into two main parts. We will give

a brief introduction to the specific system at the beginning of each respective chapter. In chapter 2, we consider the change of Laughlin state defined on the torus with regard to the modular parameter τ that parametrizes the geometry of the torus. Our results connect to geometry in two essential ways. First, we obtain new results on a class of exactly solvable one dimensional lattice Hamiltonians related to the system and parameterized by τ . This is achieved by systematically studying in the evolution of the system as a function of τ (or equivalently, the underlying metric of the torus) into the simple thin torus limit. This will also result in a new “guiding-center-only” presentation of the famous Laughlin states. On the other hand, the Berry phase of the system over the complex τ plane also has a physical meaning, as it is connected to the so called “Hall viscosity” of the state. [2, 48, 51] We will explore this connection by exposing its relation to our generator of the τ evolution of the state, and thereby giving a numerical application of the latter. In chapter 3, we study the Berry phase of magnetic vortices in a 2D lattice model of a type II superconductor. Here we adiabatically evolve the system by moving the vortex around. We find the Berry curvature to be very interesting in various aspects, and suggesting (and some case rigorously establishing) bosonic statistics of the vortex. In chapter 4 we summarize the thesis and conclude. There are also various appendices explaining some detail aspects of this thesis.

Chapter 2

Heat equation approach to geometric changes of the torus Laughlin state

2.1 Introduction to Quantum Hall Effect

The integer quantum Hall effect is a remarkable discovery made in 1980 by von Klitzing et al [30]. It is a macroscopic quantum phenomenon which occurs in 2D electron systems at low temperature and strong magnetic field. It is characterized by the famous quantization of Hall conductance, which appears as plateaus at integer multiples of e^2/h . The quantized conductance is so accurate that the mass in the SI unit may soon be redefined in term of the von Klitzing constant $R_K = h/(2e)$ and Josephson constant. This great accuracy also shows the robustness of the quantum Hall effect, in the sense that it is totally indifferent to impurities and the detailed geometry of the 2D samples. Two years later, Tsui et al. [63] discovered the fractional quantum Hall effect with fractional quantization of Hall conductance of high mobility samples in 1982. These two great discoveries won the Nobel prize separately

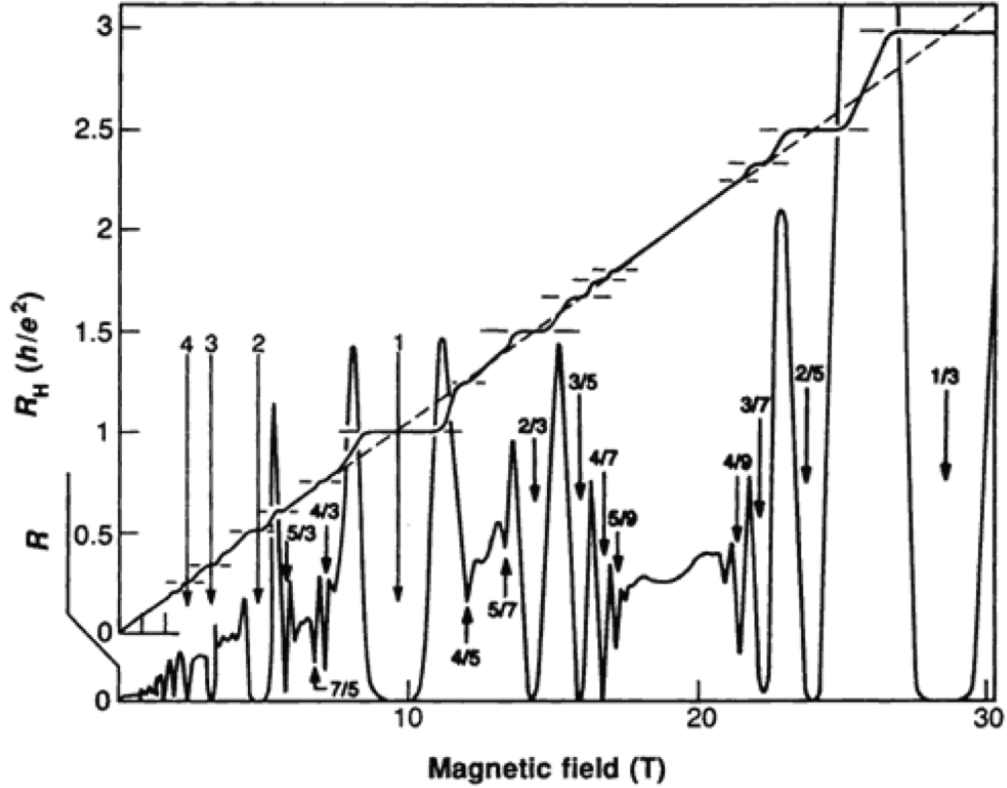


Figure 2.1: Experimental result of integer and fractional quantum Hall effect

in 1985 and 1998. Fig. 2.1 shows the experimental result taken from Ref. [74]. It is easy to see the fascinating feature of integer and fractional quantization of Hall conductance.

Below we will introduce the theoretical basis of the quantum Hall effect, which is also the basis for the research presented later in this chapter.

2.1.1 2D electron gas in a magnetic field

In order to understand the quantum Hall effect, we first need to know the dynamics of electrons in a magnetic field. We begin with a semi-classical picture.

Classically, electrons move in cyclotron orbits in the presence of a uniform perpendicular magnetic field. This is governed by the simple equation, $m_e v \omega_c = Bev$, where e is electron charge, m_e is the mass of electron, ω_c is the cyclotron frequency, B is the magnetic field and

v is the magnitude of the velocity. We introduce the semi classical quantization condition,

$$B \cdot \pi r^2 = nh/e, \quad (2.1)$$

which means that the flux through the orbit is quantized as integer multiples of the flux quanta $\Phi_0 = h/e$. According to our discussion about AB phase in chapter 1, we can understand that this condition allows the electron to interference constructively with itself. Note that this is a first occurrence of Berry phase in our discussion of quantum Hall physics. Then it is easy to write down the quantized energy of the electron,

$$E_n = \frac{1}{2}mv^2 = n\hbar\omega_c, \quad (2.2)$$

where $v = r\omega_c$ is used. When compared with the following quantum mechanical theory, this semi-classical theory has the right energy spectrum except for the zero point energy $\hbar\omega_c/2$.

Quantum mechanically, the Hamiltonian for a 2D electron in constant magnetic field is as follow,

$$H = \frac{1}{2m_e}(\hat{p} - e\mathbf{A})^2. \quad (2.3)$$

Here \hat{p} is the canonical momentum, \mathbf{A} is the magnetic vector potential. We neglect the spin degree of freedom because the Zeeman effect favors the spin alignment with the strong magnetic field. In the symmetric gauge, the magnetic vector potential for constant magnetic field is $\mathbf{A} = (-By/2, Bx/2, 0)$. Then the dynamic momentum $\boldsymbol{\pi} = \mathbf{p} - e\mathbf{A}$ satisfies the commutation relation $[\pi_x, \pi_y] = -i\hbar^2/l_B^2$, where the magnetic length is $l_B = \sqrt{\hbar/|e|B}$. We can also introduce the corresponding classical coordinate of the cyclotron motion center, or

guiding center,

$$\mathbf{R} = (X, Y) = \left(x - \frac{l_B^2}{\hbar}\pi_y, y + \frac{l_B^2}{\hbar}\pi_x\right). \quad (2.4)$$

They satisfy similar commutation relation $[X, Y] = il_B^2$, and also commute with the dynamic momentum, $[\boldsymbol{\pi}, \mathbf{R}] = 0$.

Thus we can construct two ladder operators,

$$a = \frac{l_B}{\sqrt{2}\hbar}(\pi_x - i\pi_y), \quad (2.5)$$

$$b = \frac{1}{\sqrt{2}l_B}(X + iY). \quad (2.6)$$

They satisfy the bosonic commutation relations $[a, a^\dagger] = 1$ and $[b, b^\dagger] = 1$. With the help of these ladder operators, the Hamiltonian and angular momentum can be written into the following “2nd quantized” form,

$$H = \hbar\omega_c\left(a^\dagger a + \frac{1}{2}\right), \quad (2.7)$$

$$L_z = \hbar(a^\dagger a - b^\dagger b), \quad (2.8)$$

where ω_c is the same cyclotron frequency in the semi classical picture.

The common eigenstate for an electron is given by 2 positive quantum numbers n and m , with $a^\dagger a|n, m\rangle = n|n, m\rangle$, and $b^\dagger b|n, m\rangle = m|n, m\rangle$. The wave function of the $|0, 0\rangle$ state can be solved by the fact that it is annihilated by both a and b operators.

$$\phi_{0,0}(\mathbf{r}) = \frac{1}{\sqrt{2\pi}l_B} \exp\left(-\frac{r^2}{4l_B^2}\right) = \frac{1}{\sqrt{2\pi}l_B} \exp\left(-\frac{|z|^2}{4}\right),$$

Here we introduce the complex coordinates $z = (x - iy)/l_B$, which will be convenient in later calculation.

Then all the other eigenstates are derived by applying a^\dagger and b^\dagger to the $|0, 0\rangle$ state as follows,

$$\phi_{n,m}(\mathbf{r}) = \frac{a^\dagger}{\sqrt{n!}} \frac{b^\dagger}{\sqrt{m!}} \phi_{0,0}(\mathbf{r}).$$

One can see from Eq. 2.7 and 2.8 that n is the energy quantum number, and $n-m$ is the angular momentum quantum number. We see that states are largely degenerate. States with the same energy constitute the Landau levels. Among these, the lowest Landau level (LLL), where $n=0$, is what we will study later on in this chapter.

$$\phi_{0,m} = \frac{1}{\sqrt{2\pi 2^m m!} l_B} z^m e^{-|z|^2/4}. \quad (2.9)$$

The lowest Landau level has many interesting properties. The probability of $\phi_{0,m}$ localizes in a ring shape with radius $\sqrt{2m}l_B$. The expectation value of r^2 is $\langle r^2 \rangle = 2(m+1)l_B^2$, indicating that every electron state takes an ring shape area of $2\pi l_B^2$. This is also true for higher Landau levels. Interestingly, the magnetic flux through the area that every electron state takes is $2\pi l_B^2 B = h/e \equiv \Phi_0$, where Φ_0 is again the magnetic flux quantum. Here it comes a simple conclusion, there is one electron state corresponding to each flux quantum for every Landau level.

As we pointed out, the lowest Landau level is localized circularly. The phase around the circle is $2\pi m$ according to Eq. 2.9. This is how the angular momentum is quantized. However, we can also interpret this phase as Aharonov-Bohm (AB) phase. As we discussed

in chapter 1, an electron gets AB phase when it encircles magnetic flux.

$$\text{AB phase} = \frac{e}{\hbar} \oint \mathbf{A} \cdot d\mathbf{l} = \frac{e}{\hbar} \Phi$$

Here Φ is the magnetic flux inside the closed loop. For lowest Landau level, $\Phi = 2m\pi l_B^2 B = m\Phi_0$. So the AB phase for the electron in LLL is $2\pi m$, which is the same as the angular momentum phase. Therefore, the lowest Landau level with definite angular momentum has the corresponding amount of magnetic flux inside its orbital. The situations for higher Landau levels are similar. This orbital-flux correspondence leads to a well known “flux pumping” thought experiment. If we place an additional solenoid at the origin, perpendicular to the plane, the magnetic flux can be adiabatically changed for all the states in the Landau levels. If we increase the magnetic flux by Φ_0 , the physics of electron will remain the same because this is only a gauge change with trivial gauge phase. The only difference is that all the m values are increased by 1. This notion of flux pumping is essentially related to the quantized Hall conductance, as we will now explain.

2.1.2 The integer quantum Hall effect

We briefly describe a thought experiment explaining integer quantum Hall effect. This is basically equivalent to Laughlin’s Gedankenexperiment[31, 76].

We consider an annulus of 2D electrons in Fig. 2.2 , with constant perpendicular magnetic field \mathbf{B} . The inner and outer edges of the annulus have voltage difference ΔV . We assume that the fermi energy is in the “mobility” gap so that there is no current across the annulus. This also means that Landau levels are either fully occupied or empty, hence there is no

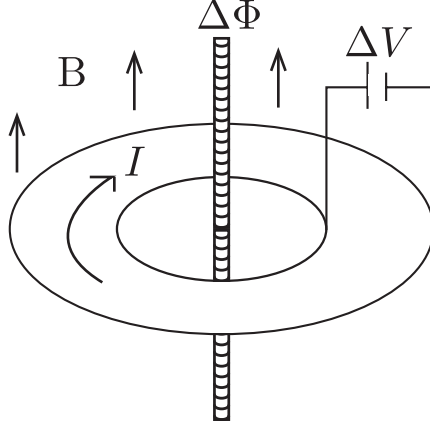


Figure 2.2: IQHE on an annulus with uniform field B . Additional solenoid is present in the center of annulus.

possibility of dissipation. We assume there are ν fully occupied Landau levels.

There is a solenoid at the center of the annulus with adjustable magnetic flux through it. As we mentioned in the last section, a change in flux by $n\Phi_0$ restores the annulus to its original quasi equilibrium state except for a $2n\pi$ gauge phase for every electron. However, electrons are transferred from one edge to the other if we change the flux adiabatically. The free energy changes by

$$\Delta F = \nu n e \Delta V.$$

Flux change $d\Phi$ also results in a voltage ϵ around the annulus. This will do the following work,

$$W = \int dt I \epsilon = \int dt I \frac{d\Phi}{dt} = n I \Phi_0.$$

The work done should be equal to the change of free energy. Thus we have,

$$\sigma_{xy} = \frac{I}{\Delta V} = \nu \frac{e^2}{h}.$$

This is the expected result for the integer quantum Hall effect. It shows that when every extended state below the fermi energy is fully occupied, the Hall conductance is quantized. With the help of defects-induced local states, the fermi level will reside within the mobility gap between Landau levels over finite ranges of magnetic field. Then the Hall plateaus are well explained.

Of course this is only a rough understanding of integer quantum Hall effect. Details about the defects, edge states, external field and temperature effect need to be considered in order to get a full description, which we will not introduce here.

2.1.3 The fractional quantum Hall effect

One may find that the Coulomb interaction between electrons is neglected in the last section on the integer quantum Hall effect. It can be assumed to be weak compared to the Landau level splitting. However the coulomb interaction is essential for fractional quantum Hall effect. The resulting energy gap is then determined by the interaction, so the state is less robust. This is also the reason that FQHE was found in high mobility samples, where electron interactions is comparable to the impurity potential.

From the knowledge of IQHE, the existence of an energy gap is essential for the quantization of Hall conductance. For the FQHE case, we can make a similar guess that the Coulomb interaction leads to splitting of Landau levels at a fractional occupation. This has been verified by exact diagonalization of Coulomb interaction in small systems [75].

Due to the quenching of kinetic energy within a Landau level, even a weak interaction dominate the physics of partially filled Landau levels and can not be treated perturbatively. However, the variational method based on Laughlin's trial wave function has proven to be

very powerful [32]. We follow the Laughlin's reasoning to arrive at the wave function named after him.

To make things simple, we first restrict the electrons to the lowest Landau level Hilbert space, where $\nu = 1/3, 1/5, 2/3, \dots$ fractions are expected to happen. As we find in Eq. 2.9, the single electron wave function in symmetric gauge has the following general form,

$$\phi(\mathbf{r}) = f(z)e^{-|z|^2/4},$$

where $f(z)$ is a polynomial in z . So the multi-electrons wave function in this Hilbert space is in general as follows,

$$\Psi(\mathbf{r}_1, \mathbf{r}_2, \dots, \mathbf{r}_N) = f(z_1, z_2, \dots, z_N)e^{-\sum_i |z_i|^2/4}.$$

We can further restrict the polynomial f to be homogenous because the total angular momentum, which is proportional to the sum of powers of z_i in each term, should be conserved by Coulomb interaction. There is also a natural restriction that f should be anti-symmetric according to Pauli principle.

Another restriction is from the nature of Coulomb interaction, which depends only on the distance between electrons. So f should be a function of inter-electron distance only. The simplest form of f is a Jastrow type function, where only two body correlation enters.

$$f(z_1, z_2, \dots) = \prod_{i>j} g(z_i - z_j).$$

With all the restrictions combined, the polynomial is fixed as $g(z) = z^q$, where q is an

odd integer. Then we arrive at Laughlin's wave function,

$$\Psi_q(\mathbf{r}_1, \mathbf{r}_2, \dots, \mathbf{r}_N) = \prod_{i>j} (z_i - z_j)^q e^{-\sum_i |z_i|^2/4}. \quad (2.10)$$

Laughlin wave function is a great success, especially in the sense that it's only an ansatz. It captures nearly all the essential features of $1/3$ fractional electron states although the exact interaction is not Coulomb type, as we will see in Section 2.1.4. It is the starting point of all the other trial wave functions.

I was gladly informed by Prof. Clark during the defense that the Laughlin states, which I am dealing with a lot, has some relation with the Wayman Crow Professor of Physics at Washington University, Eugene Feenberg. Robert Laughlin made an acknowledgement of Eugene Feenberg's Jastrow ground state in his Nobel bibliography, saying that it was Eugene Feenberg's book, which connected his guess to one-component plasma. I have enjoyed 5 years of the distinguish Eugene Feenberg Memorial Lectures. Until in the end, I realized this mystery relationship, which I would call "Yinyuan" in Buddhism language. That is, some hidden cause is always around, but people won't find it and realize its importance until the very moment.

The Laughlin states have occupation number $\nu = 1/q$ in the thermodynamic limit. Here we emphasize that the occupation number is the ratio of electrons to the total flux quanta. As we showed before, the flux can be changed, so that the occupation number will deviate from $1/q$ slightly. This process can be understood as introducing of finite size quasiparticles.

Let us first look at the state in which the Laughlin state is multiplied by all the z_i ,

$$\prod_i z_i \Psi_q \propto \prod_i b_i^\dagger |\Psi_q\rangle.$$

If one expand the Laughlin state into polynomials, in every term the power of z_i is increased by 1. This is reminiscent of our earlier discussion of adiabatic flux pumping. The effect is the same as if a flux quantum Φ_0 was introduced in the origin by an infinitesimal solenoid. In a region near the origin, the amplitude of the electron wave function decreases. So there appears some positive charge around the origin. This can be considered as a quasiparticle.

There is nothing special for the origin in the infinite 2D plane. We can introduce such quasiparticles at any coordinate z_0 . If q quasiparticles are introduced, the wave function becomes,

$$\prod_i (z_i - z_0)^q \Psi_q.$$

This is the Laughlin state with one extra electron fixed at z_0 . In other words, q quasiparticles are neutralized by one electron. So the charge of a quasiparticle is fractional, $e^* = -e/q$. This is usually called a quasi-holes because of positive fractional charge.

Similarly, a negative charge quasielectron can be introduced at the origin by decreasing the flux by Φ_0 . The wave function of the quasielectron is

$$\prod_i [e^{-|z_i|^2/4} \frac{\partial}{\partial z_i} e^{|z_i|^2/4}] \Psi_q \propto \prod_i b_i |\Psi\rangle.$$

Again we can replace the origin with a fixed coordinate z_0 by replacing the derivative with $(2\frac{\partial}{\partial z_i} - z_0^*)$. Quasielectrons are just anti-particle of quasiholes, with fractional charge e/q .

Laughlin states are quite good approximations to the exact ground states of FQHE at filling factor $1/q$ [12]. However, there are obvious plateaus at other filling factor p/q experimentally. These fractions can be understood by a hierarchy theory proposed by Haldane, Laughlin and Halperin [19, 26] or the composite fermion picture of Jain [29]. While the electrons form Laughlin states at some circumstance, the quasiparticles emerged in Laughlin states, can interact with each other and form Laughlin states of quasiparticles at appropriate densities. It has been shown that fractions such as $2/5$, $3/7$ and $4/9$ is successfully explained by the hierarchy theory. Some other FQH states such as filling factor $2/3$, $3/5$ are nothing more than the particle-hole inversion of $1/3$ and $2/5$ states.

The occupation number ν can be fractional due to the fact that fractionally charged quasi-particles may be transported in the adiabatic pumping flux argument, as the additional quasiparticles will be trapped at the local impurity sites.

2.1.4 Haldane's pseudopotential

The concept of pseudopotentials was first introduced by Haldane [19]. It becomes a extremely powerful tool in quantum Hall physics. It suggests special model Hamiltonians that have exactly solvable ground states as we will show in the following.

Haldane's pseudopotential is defined as the energy cost for two electrons to have a given relative angular momentum. These pseudopotentials give a complete description of a generic two body interaction $V(|\mathbf{r}_1 - \mathbf{r}_2|)$, which is rotationally and translationally invariant, through the LLL Hilbert space. The relative wave function where two electrons i, j has relative angular momentum $m\hbar$ is $\psi_m(\mathbf{r}_i, \mathbf{r}_j) \propto z^m \exp(-|z|^2/8)$, where $z = z_i - z_j$ is the

relative coordinate. According to the definition, the pseudopotential V_m is given as follows,

$$\langle \psi_m | V(|\mathbf{r}_i - \mathbf{r}_j|) | \psi'_m \rangle = V_m \delta_{m,m'}$$

Due to the antisymmetry of the wave function, V_m is non-zero only for odd m . Because the interaction will preserve angular momentum conservation, it is specified by only the diagonal part of the matrix element, which is a minimal description. So the interaction can be written in the following form,

$$H = \sum_{i>j} V(\mathbf{r}_i - \mathbf{r}_j) = \sum_n \sum_{i>j} |\psi_{2n+1}(\mathbf{r}_i, \mathbf{r}_j)\rangle V_{2n+1} \langle \psi_{2n+1}(\mathbf{r}_i, \mathbf{r}_j)|. \quad (2.11)$$

Model Hamiltonians can be built by choosing explicit values for the parameters V_{2n+1} . The most simple example is given by setting $V_l = 0$, for all $l > 1$, namely only the V_1 term remain positive. This turns out to be a very simple repulsive interaction,

$$V_1(r) = \nabla_z^2 \delta^2(z). \quad (2.12)$$

It is basically a hard core repulsion interaction which is exactly solvable. For Laughlin state at filling factor $\nu = 1/3$, there is no pairs of electrons with relative angular momentum \hbar . Clearly the above interaction will annihilate the $q = 3$ Laughlin states. Actually it is the unique ground state of V_1 in LLL Hilbert space with filling factor $1/3$ [19].

Similar model Hamiltonians can be constructed for other Laughlin states with $\nu = 1/q$ by setting $V_l = 0$ for $l \geq q$, and $V_l > 0$ for $l < q$.

2.2 Motivations

In the last section, we have discussed the technical basis for understanding the QHE. We have seen that the Laughlin states are very successful special wave functions that paved the way for further theoretical developments. There are many other special wave functions [41, 50, 24, 26, 59] that describe other fractional states. These “wave function” approaches are greatly enhanced by the construction of parent Hamiltonians. [50, 24, 19, 62, 18] This very particular class of quasi-solvable¹ Hamiltonians consists of Landau level projected ultra-local interactions, which enforce the analytic properties that uniquely characterize the respective ground state. The prime example for such a parent Hamiltonian is given by the V_1 -pseudopotential,[19] as we discussed in section 2.1.4. Its unique ground state at filling factor $\nu = 1/3$ is the Laughlin state corresponding to this filling.

Due to the Landau level projection, the pseudo-potential Hamiltonian acts only on the “guiding center” degrees of freedom, which exhaust the large degeneracy within a given Landau level, and commute with the generators of inter-level transitions. (The latter are related to the kinetic momenta of the particles, see section 2.1.1) It is therefore beneficial to make the action of the Hamiltonian on guiding center variables manifest. This is in particular the case when the Hamiltonian is expressed using creation/annihilation operators for a set of eigenstates, say, of one of the two non-commuting guiding center components in Eq. 2.4, which form a basis for the LLL. In numerics, such a second quantized “guiding center” description of the Hamiltonian is essential to make use of the reduced Hilbert space dimensionality owing to the LLL projection.

¹By this we mean that the ground state is exactly known.

Previous work on Jack polynomials has provided a general rule to construct the guiding center representation of some special wave functions in the plane, sphere and cylinder geometries. [7, 6] However things are quite different on the torus because the Jastrow factor appearing in these special wave functions are no longer of polynomial form so that the Jack polynomial approach does not work on the torus. Here, we would like to explore the possibility of constructing the guiding center representations by adiabatically evolving from the thin torus limit, which is simple and well known[55]. We manage to find the generator for adiabatic evolution in geometric parameter τ , which makes the guiding center representation available for general tori. Further more, this generator is also intimately related to the geometric phases that defines the Hall viscosity. The following part of this chapter has been published in Ref. [77].

2.3 Guiding center representation of Laughlin state, from cylinder to torus

We illustrate the guiding center representation for the cylinder geometry first, for reasons that will soon become apparent. We introduce a set of LLL basis states as described above, given by:

$$\phi_n(z) = \xi^n e^{-\frac{1}{2}x^2} e^{-\frac{1}{2}n^2/r^2} \quad (2.13)$$

where $\xi = e^{z/r}$ is an analytic function of $z = x+iy$ that satisfies periodic boundary conditions in y , appropriate for a cylinder of perimeter $2\pi r$ (using Landau gauge, $\mathbf{A} = (0, x)$). These orbitals are eigenstates of the x-component of the guiding center with eigenvalues n/r , where,

for the time being, we set the magnetic length l_B equal to 1. The 1/3-Laughlin state on the cylinder is then expressed as[52]

$$\psi_{1/3}(z_1 \dots z_N) = \prod_{i < j} (\xi_i - \xi_j)^3 \times e^{-\frac{1}{2} \sum_k x_k^2}. \quad (2.14)$$

With respect to the basis Eq. (2.13), the V_1 pseudo-potential takes on the following second quantized form (cf, e.g., Ref. [33]):

$$\begin{aligned} \hat{V}_1 &= \sum_R Q_R^\dagger Q_R \\ Q_R &= \sum_x x \exp(-x^2/r^2) c_{R-x} c_{R+x} \end{aligned} \quad (2.15)$$

In the first line, the sum goes over both integer and half-odd integer values of R , whereas in the second it goes over integer (half-odd integer) if R is integer (half-odd integer), such that labels $R \pm x$ are then always integer.

The one parameter family of models (2.15) share many features with one-dimensional (1D) lattice models that arise elsewhere in solid state physics, such as translational invariance and short ranged (exponentially decaying) interactions. It is thus not surprising that it has recently been proposed to be of use in the absence of (proper) Landau level physics, e.g., in flat band solids both with[46] and without[70] non-zero Chern numbers, and in quite general terms in Ref. [55].

Despite the usefulness of the second quantized description (2.15) of the pseudo-potential, it would be very difficult to solve for the zero energy eigenstates of the model in this form, or to even know analytically that such zero energy eigenstates exist. For this we rely on the

original first-quantized definition of the pseudo-potential \hat{V}_1 , and on the explicitly known analytic form of the Laughlin state, Eq. (2.14), in terms of ordinary position variables. It would be highly non-trivial, however, to come up with such a first quantized language for the problem Eq. (2.15) if its connection to LLL orbitals were not a priori known. This is so because this language becomes available only after proper embedding of the degrees of freedom associated with the operators c_n, c_n^\dagger in Eq. (2.15) into a larger Hilbert space. In Eq. (2.15), no information is retained about the kinetic momenta that determine the structure of the Landau levels. Indeed, as Haldane has recently shown,[22] by making these kinetic momenta subject to a different metric from that entering the interactions, one obtains a different way to naturally embed the problem (2.15) into the larger Hilbert space of square integrable functions. In this setup, Eq. (2.15) remains unaltered, but the resulting wave function loses the analytic properties of Eq. (2.14) that make the problem tractable.[22, 47] Moreover, the solid state applications mentioned initially represent yet another way to embed the problem (2.15) into a larger Hilbert space.

These considerations show that “interaction only” models such as (2.15), especially ones that share the “center-of-mass conserving” property,[55] may enjoy a considerable range of applications, but at the same time, may be quite hard to solve in general.² This is chiefly due to the fact that the Laughlin state, in its second quantized/guiding center presentation, is quite a bit more complicated than in its analytic first quantized form Eq. (2.14). While no closed form seems to be known for the amplitudes $\langle 0|c_{n_1} \dots c_{n_N}|\psi_{1/3}\rangle$, much progress has recently been made in understanding their structure for the cylinder geometry, and

²We note though a tractable truncated version of Eq. (2.15) with matrix product ground state given in Ref. [42].

for any other geometry in which the analytic part of Laughlin's wave function is given by a polynomial. Indeed, for Laughlin states and many other quantum Hall trial wave functions, these polynomials have been identified as Jack polynomials, multiplied by Jastrow factors.[7, 6] This allows the amplitudes $\langle 0|c_{n_1} \dots c_{n_N}|\psi_{1/3}\rangle$ to be determined recursively. For the cylinder Laughlin state, this can be sketched as follows. We consider the expansion of Eq. (2.14) into monomials,

$$\psi_{1/3}(z_1 \dots z_N) = \sum_{\{n_k\}} C_{\{n_k\}} \prod_k \xi_k^{n_k} e^{-\frac{1}{2}x_k^2} \quad (2.16)$$

The product in the above equation can be interpreted as a state with definite single particle occupation numbers, up to a normalization. (The $C_{\{n_k\}}$ have the proper (anti)-symmetry to allow (anti)-symmetrization of the product.) This normalization is readily read from Eq. (2.13). We thus have[52]

$$|\psi_{1/3}\rangle_r = \sum_{\{n_k\}} e^{\frac{1}{2r^2} \sum_k n_k^2} C_{\{n_k\}} c_{n_N}^\dagger \dots c_{n_1}^\dagger |0\rangle. \quad (2.17)$$

The monomial coefficients do not depend on r , and are known recursively, starting from the coefficient of the ‘‘root configuration’’ $c_{n_N}^\dagger \dots c_{n_1}^\dagger |0\rangle = |10010010010\dots\rangle$ through a process known as ‘‘inward squeezing’’.[7, 6]

A remarkable aspect of Eq. (2.17) is that the dependence on geometry, in this case the cylinder radius r , comes in only through the trivial normalization factor. This is matched by a similarly trivial r -dependence of the interaction \hat{V}_1 . It is quite easy to see that the condition that the Hamiltonian Eq. (2.15) has a zero energy eigenstate (which, by positive

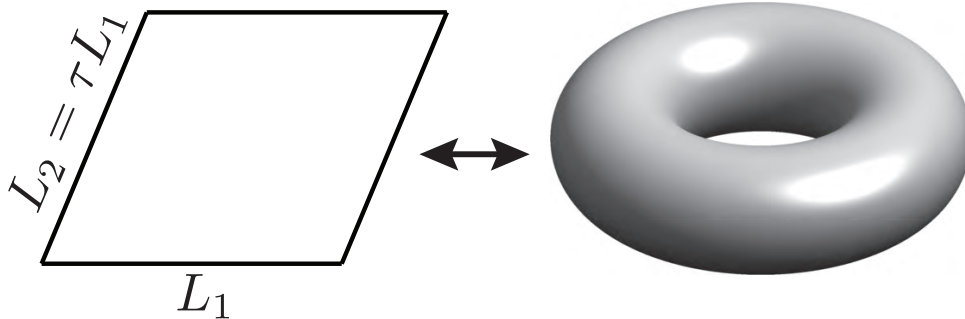


Figure 2.3: Fundamental domain for torus wave functions.

semi-definiteness, must be a ground state), which reduces to $Q_R|\psi_{1/3}\rangle_r = 0 \forall R$, yields an r -independent condition on the coefficients $C_{\{n_k\}}$. In this way it becomes manifest that regardless of the value of r , one is always solving the same problem, which is intuitively clear from the simple analytic form of the Laughlin wave function (2.14) and its trivial r -dependence. It should also be emphasized that the simple r -dependence of Eq. (2.17) is not particular to the Laughlin state. It is a direct consequence of the polynomial form of the wave function, and carries over without change to any quantum Hall trial state on the cylinder.

The situation is rather different for the torus geometry. The main purpose of this work will be to get a handle on the guiding center presentation of the torus Laughlin states. In the remainder of this introduction, we review some well known facts that make life more complicated on the torus.

In first quantized language, we pass to the torus by introducing periodic boundary conditions in the complex plane along two fundamental periods L_1 and L_2 , where L_1 is taken to be real, and $\text{Im}L_2 > 0$ (Fig. 2.3). The geometry of the torus can be parameterized by $\tau = L_2/L_1$, the modular parameter.

The LLL basis on torus can be known from symmetrization of LLL basis on cylinder

according to magnetic translation. It can be written into the following theta function form,

$$\chi_l(z) \propto e^{\frac{1}{2}y^2} \theta \begin{bmatrix} l/L \\ 0 \end{bmatrix} (Lz/L_1, L\tau). \quad (2.18)$$

Here $l = 0, 1, 2, \dots, L - 1$, is the label indicating the degeneracy of LLL on torus. $L = L_1 \text{Im} L_2 / (2\pi)$ is the number of flux quanta penetrating the surface of the torus. $\theta \begin{bmatrix} a \\ b \end{bmatrix} (z, \tau)$ is the Jacobi theta function of characteristics a and b .

$$\theta \begin{bmatrix} a \\ b \end{bmatrix} (z, \tau) = \sum_m e^{i\pi\tau(m+a)^2 + 2i\pi(m+a)(z+b)}.$$

The basis has the following periodic condition:

$$\frac{\chi_l(z + L_1)}{\chi_l(z)} = 1 \quad (2.19)$$

$$\frac{\chi_l(z + L_2)}{\chi_l(z)} = e^{-i\pi L\tau - 2\pi i Lz} \quad (2.20)$$

Under magnetic translation, the basis evolve as follows,

$$T_1 \chi_l(z) = \chi_l(z + \frac{1}{L}) = e^{2\pi i \frac{l}{L}} \chi_l(z) \quad (2.21)$$

$$T_2 \chi_l(z) = e^{-2\pi i x} \chi_l(z - \frac{\tau}{L}) \propto \chi_{l-1}(z) \quad (2.22)$$

Here T_i stand for magnetic translation of L_i/L along L_1 or L_2 direction. It clear that the LLL states return to itself after magnetic translation of L_1 and L_2 .

The Laughlin state at general filling factor $1/q$ then becomes[23]

$$\psi_{1/q}^\ell(z_1 \dots z_N) = \exp\left(-\frac{1}{2} \sum_k y_k^2\right) F^\ell(Z, \tau) \prod_{i < j} \theta_1\left(\frac{z_i - z_j}{L_1}, \tau\right)^q \quad (2.23)$$

Here, $\theta_1(z, \tau)$ is the odd Jacobi theta-function, and for the factor depending on the “center of mass” $Z = z_1 + \dots + z_N$, which also depends on an additional label $\ell = 0 \dots q-1$ corresponding to a choice of basis in the q -fold degenerate[72] ground state space, we adopt the convention of Ref. [49]:

$$F^\ell(Z, \tau) = \theta \left[\begin{array}{c} \frac{\ell}{q} + \frac{L-q}{2q} \\ -\frac{L-q}{2} \end{array} \right] (qZ/L_1, q\tau). \quad (2.24)$$

Thus, while the Laughlin state is still of the general form of a Gaussian factor multiplying an analytic function in the complex particle coordinates z_i , the latter is not of polynomial form. As a result, to the best of our knowledge, there is currently no detailed understanding of the structure of the guiding center description of this state. By this we mean a general understanding of the coefficients of the analog of Eq. (2.17):

$$|\psi_{1/3}^\ell\rangle_\tau = \sum_{\{n_k\}} C_{\{n_k\}}^\ell(\tau) c_{n_N}^\dagger \dots c_{n_1}^\dagger |0\rangle. \quad (2.25)$$

In particular, the τ -dependence of the coefficients $C_{\{n_k\}}^\ell(\tau)$ is *not* of a simple form reminiscent of the r -dependence explicit in Eq. (2.17). Moreover, intuitively, one would still expect that these coefficients can be generated from the dominance pattern, i.e., 100100100... at $\nu = 1/3$. Indeed, this configuration is still dominant on the torus, in the sense that it is the configuration that dominates in the thin torus limit[55, 3, 56, 4]. The success of the

thin torus approach in determining physical properties, such as Abelian and non-Abelian statistics[57, 53, 14, 15] and the presence of gapless excitations[58], suggests that even on the torus these patterns allow for a reconstruction of the full many-body wave function. On the other hand, there is no notion of “inward” squeezing on the torus, due to periodic boundary conditions. The main result of this chapter will be the development of a machinery for the above mentioned reconstruction of the full torus Laughlin state in the guiding center description, from the thin torus state. Since as an additional complication, such machinery can be expected to depend non-trivially on τ , we first focus our attention on the dependence of the coefficients $C_{\{n_k\}}^\ell(\tau)$ on the geometric parameter.

As a final remark, we point out[23] that the torus Laughlin states at $\nu = 1/3$ are still the unique ground state of the V_1 pseudo-potential. Its second quantized form agrees with a straightforward periodization of the model (2.15), with

$$Q_R = \sum_{\substack{0 < x < L/2 \\ x+R \in \mathbb{Z}}} \sum_{m \in \mathbb{Z}} (x + mL) \exp\left[\frac{2\pi i \tau}{L}(x + mL)^2\right] c_{R-x} c_{R+x}. \quad (2.26)$$

One sees that for $\tau = i|L_2|/2\pi r$, $L_2 = iL/r$, this reduces to the cylinder form Eq. (2.15) for $L \rightarrow \infty$, and respects the periodic boundary condition $c_n = c_{n+L}$ otherwise. (Eq. (2.26) is valid for general complex τ , though). One therefore passes from Eq. (2.15) to Eq. (2.26) (with imaginary τ) through straightforward introduction of periodic boundary conditions (PBCs). Yet the solution of Eq. (2.26) is arguably much less under control. The introduction of PBCs is a standard and very useful tool throughout solid state physics. We thus expect that a better understanding of the guiding center description of the torus Laughlin state will also benefit the solid state applications[70, 46] mentioned initially.

The remainder of this chapter is organized as follows. In section 2.4 we construct a two-body operators that generated the changes in the guiding center variables of the torus Laughlin state with modular parameter τ . Sections 2.4.1 and 2.4.2 highlight further formal similarities and differences between the cylinder and the torus. Sec. 2.4.3 presents the heat equation for the τ -derivative of the analytic Laughlin state. Sec. 2.4.4 introduces a 2D to 1D mapping, which is our device for embedding lowest Landau levels at different modular parameter τ into the same larger Hilbert space. In Sec. 2.4.5 we derive the generator mentioned above. In Sec. 2.4.6 we symmetrize this operator and present a byproduct of this study, a hitherto unknown class of two-body operators that annihilate the torus Laughlin state. In Sec. 2.4.7 we postulate a presentation of the torus Laughlin state in terms of its thin torus, or “dominance” pattern, and the class of two-body operators generating changes in geometry. In Sec. 2.5 we demonstrate the postulate of Sec. 2.4.7 numerically, and work out the relation of our generator with the Hall viscosity[48], which we calculate numerically as a demonstration of analytical results, comparing the resulting data to earlier numerical studies. We discuss our results in Sec. 2.6. We also have Appendix in the end of the thesis discussing some technical details.

2.4 Construction of the 2-body operator

2.4.1 A final look at the cylinder case

As motivated above, to establish a machinery that generates the full guiding center description of the Laughlin state from the root configuration, a natural starting point is to get under control how this description changes with the geometric parameter τ . To this end, we

will seek to construct an operator that generates changes of the guiding center degrees of freedom to first order in $d\tau$. The similar problem for the cylinder, where r is the geometric parameter, is comparatively trivial and was already addressed in the introduction. For later reference, it is instructive to first cast these results in terms of a generator of infinitesimal changes in the parameter r^{-2} . Eq. (2.17) can be written as

$$|\psi_{1/3}\rangle_{r'} = e^{(r'^{-2}-r^{-2})G_{r^{-2}}}|\psi_{1/3}\rangle_r \quad (2.27)$$

where

$$G_{r^{-2}} = \frac{1}{2} \sum_n n^2 c_n^\dagger c_n \quad (2.28)$$

is the generator of changes in the geometric parameter r^{-2} . Note that it is independent of r . We emphasize again that (2.27), (2.28) are very general, and apply to other quantum Hall trial states on the cylinder as well. In writing (2.27), we leave it understood that the exponentiated operator generates the change of the guiding center degrees of freedom only; it does not generate in any way the change of the LLL orbitals themselves as a function of r , Eq. (2.13). We are only concerned here with the change in guiding center degrees of freedom, since the object of study is the second quantized Hamiltonian Eq. (2.15), in which degrees of freedom associated with kinetic momenta are not retained. We will thus carefully distinguish from now on between the Laughlin wave function $\psi_{1/3} \equiv \psi_{1/3}(z_1 \dots z_N; r)$, which lives in the full Hilbert space of square integrable functions over some domain, and the ket $|\psi_{1/3}\rangle_r$, which lives in an abstract Hilbert space denoted \mathcal{L} that is isomorphic to the LLL for any given value of cylinder radius r . Similar conventions will be used below for the torus. In \mathcal{L} , therefore, all those orbitals with the same guiding center quantum number n become

identified, which originally belonged to different LLLs corresponding to different values of the parameter r .³

We note that a similarly universal operator that generates changes of the guiding center degrees of freedom in response to a change in geometry can be obtained on the plane.[51, 47] Here, since a geometric deformation by means of uniform strain does not affect boundary conditions, such a deformation is implemented by a change in the metric, and unlike in Eq. (2.27), the operation implementing this deformation is unitary.

On the other hand, it is worth pointing out that in (2.27), the lack of unitarity leads to a breakdown of the equation in the “thin cylinder” limit $r \rightarrow 0$, in which $|\psi_{1/3}\rangle_r$ approaches $|100100100\dots\rangle$. The equation remains valid for arbitrarily small but finite r , where the limiting state $|100100100\dots\rangle$ receives arbitrarily small corrections, which are, however, important and may not be dropped, since they become large under the non-unitary evolution facilitated by the exponential operator. This is immediately clear from the fact that the thin cylinder state is an eigenstate of the one-body operator in the exponent. This operator is thus not capable of generating the off-diagonal matrix element needed to “squeeze” the full many-body wave function out of the thin cylinder state, i.e., the root configuration. Eq. (2.27) is thus *not* a tool to generate the full cylinder Laughlin state out of the root configuration. For the cylinder, however, other such tools are already available, as mentioned in the Introduction.[7, 6]

³Indeed, as formulated at present, these different Landau levels do not even live in the same Hilbert space, since the domain of the underlying wave functions depends on the value of r . This is inconsequential at present, however, and will later be remedied.

2.4.2 General considerations for the generator on the torus

We desire to construct an operator analogous to G_{r-2} for the torus Laughlin state, which generates changes in the guiding center variables of the state in τ . This operator is thus defined by the following equation:

$$\nabla_\tau |\psi_{1/q}^\ell(\tau)\rangle = \mathbf{G}_\tau |\psi_{1/q}^\ell(\tau)\rangle. \quad (2.29)$$

Here, \mathbf{G}_τ denotes the operator valued two-component object (G_{τ_x}, G_{τ_y}) , and $\nabla_\tau \equiv (\partial_{\tau_x}, \partial_{\tau_y})$. Note that we require that \mathbf{G}_τ is *independent* of the label ℓ distinguishing the q degenerate Laughlin states $|\psi_{1/q}^\ell(\tau)\rangle$, at given filling factor $1/q$ and given τ .

To highlight considerable differences with the similar problem on the cylinder, we now show that it follows easily from these assumptions that, unlike for the cylinder, the components of \mathbf{G}_τ *cannot* be one-body operators. For, if $G_{\tau_{x,y}}$ were one-body operators, we could symmetrize each with respect to the magnetic translation group. After symmetrization, $G_{\tau_{x,y}}$ would still satisfy Eq. (2.29). This follows from the observation that \mathbf{G}_τ was assumed to be independent of ℓ , and that the Laughlin states $|\psi_{1/q}^\ell(\tau)\rangle$ are closed under magnetic translations. However, the only one-body operator that is invariant under magnetic translations is, up to constants, the particle number operator \hat{N} . Since the $|\psi_{1/q}^\ell(\tau)\rangle$ are eigenstates of \hat{N} , it is clear that no such operators could satisfy Eq. (2.29).

In the following, we will, however, show that $G_{\tau_{x,y}}$ can be a two-body operator.

2.4.3 Heat equation for the torus Laughlin state

We begin by deriving a differential equation for the τ evolution of the analytic Laughlin wave function Eq. (2.23). We have

$$\partial_\tau \psi_{1/q}^\ell = e^{-\frac{1}{2} \sum_k y_k^2} ((\partial_\tau F^\ell) f_{rel} + F^\ell \partial_\tau f_{rel})$$

where f_{rel} denotes the theta-function Jastrow factor in Eq. (2.23) and $\partial_\tau = \frac{1}{2}(\partial_{\tau_x} - i\partial_{\tau_y})$. The center-of-mass factor in the form Eq. (2.24) is also given by a theta function. Independent of ℓ , it satisfies the “heat equation”

$$\partial_\tau F^\ell(Z, \tau) = \frac{1}{4\pi i q} \partial_Z^2 F^\ell(Z, \tau) = \frac{1}{4\pi i q} \partial_X^2 F^\ell(Z, \tau) \quad (2.30)$$

with $X = \text{Re } Z$. Since ∂_X leaves the relative part invariant, the operator $(4\pi i q)^{-1} \partial_X^2$ acting on the torus Laughlin state produces just the first term above in $\partial_\tau \psi_{1/q}$. The latter can thus be expressed as

$$\partial_\tau \psi_{1/q}^\ell = \left[\frac{1}{4\pi i q} \partial_X^2 + q \sum_{i < j} \frac{\partial_\tau \theta_1(z_i - z_j, \tau)}{\theta_1(z_i - z_j, \tau)} \right] \psi_{1/q}^\ell. \quad (2.31)$$

It is pleasing that the differential operator on the right hand side of the above equation has the form of a two-body operator. There are, however, two remaining obstacles before we can express the change of guiding center variables in terms of a two-body operator derived from the above equation. First, as defined thus far, the Laughlin states Eq. (2.23) for different parameter τ do not live in the same Hilbert space. In particular, for fixed τ the state (2.23) is usually viewed as a member of the Hilbert space of square integrable functions over the fundamental domain in Fig. 2.3. In order to view the differential operator in Eq. (2.31) as an

operator in some Hilbert space, we must therefore first embed all Laughlin states for different τ , in fact all the corresponding lowest Landau levels, into the same Hilbert space, since our differential operator can be viewed as connecting states with infinitesimally *different* τ . The second obstacle is that even with such embedding, the lowest Landau level will depend on τ , i.e., will correspond to a different subspace of the larger Hilbert space \mathcal{H} (to be defined below) for different τ . The differential operator in Eq. (2.31) therefore not only describes the change of guiding center degrees of freedom with τ , it also describes the change of the Landau level itself, which we are not interested in. We will therefore find it necessary to extract the piece of Eq. (2.31) that acts on guiding centers only.

2.4.4 Mapping the problem to 1D

We will first address the more technical problem, which is the embedding of the torus Landau levels for different τ , denoted by \mathcal{L}_τ in the following, into the same larger Hilbert space \mathcal{H} . One natural approach that has been emphasized in the recent literature[48] is to choose an equivalent way to formulate the problem, where the fundamental domain remains unchanged and instead the metric is deformed. We will return to this point of view in Sec. 2.5, where we make connection with the Hall viscosity.

Here we will choose a different approach, which is rooted in the intuition that Landau-level-projected physics is effectively one-dimensional. One manifestation of this is the form of the “1D lattice” Hamiltonian Eq. (2.15) that governs the guiding center degrees of freedom. Another is the fact that wave functions in the LLL are entirely determined by holomorphic functions satisfying certain boundary conditions. As is well known, the values of such functions in the entire complex plane are already determined by those on (any interval on) the

real axis. For this reason we may restrict our study of the Laughlin states (2.23) to the real axis without any loss of information. Also, we find it convenient to choose $L_1 = 1$, $L_2 = \tau$ as the fundamental domain for the original two-dimensional (2D) wave functions. With this, after restriction to the real axis, all states (2.23) become elements of $\mathcal{H} = L^2[0, 1]$ of square integrable functions within the interval $[0, 1]$. We note that with these conventions, the area of the fundamental domain is not preserved as we change τ . Therefore, we must accommodate for this by changing the magnetic length accordingly, such that $\text{Im}\tau = 2\pi Ll_b^2$. This, however, results only in the following trivial modification of the wave functions (2.23),

$$\exp\left(-\frac{1}{2} \sum_k y_k^2\right) \longrightarrow \exp\left(-\frac{1}{2} \sum_k y_k^2/l_B^2\right),$$

which is inconsequential since we work at $y = 0$ in the following. Clearly, when Eq. (2.31) is now restricted to $y = 0$, the operator on the right hand side is a well defined differential operator within the Hilbert space \mathcal{H} (in the usual sense that its domain is dense in \mathcal{H} .)

A preferred basis for the LLL at given τ , both within the original 2D as well as the 1D Hilbert space, is given by the following wave functions,

$$\chi_n(z) = \left(\frac{2L}{\tau_y}\right)^{1/4} e^{-\frac{y^2}{2l_B^2}\theta} \begin{bmatrix} n/L \\ 0 \end{bmatrix} (Lz, L\tau). \quad (2.32)$$

These are eigenstates of the operator $\exp(\frac{2\pi i}{\tau_y}\pi_y)$, where π_y is the guiding center y -components. For any τ , the restriction of these orbitals to the real axis spans a different subspace \mathcal{L}_τ of the 1D Hilbert space \mathcal{H} , which is in one-to-one correspondence with the lowest Landau level at τ .

To see why the orbitals χ_n are a natural choice of basis in the present context, we observe that the mapping to the 1D Hilbert space \mathcal{H} introduces a new scalar product between wave functions, defined as usual by integration over $[0, 1]$ (instead of integration over the fundamental domain in 2D). Eq. (2.32) as written is normalized independent of n with respect to the 2D scalar product, but not with respect to the scalar product of \mathcal{H} . However, these orbitals are orthogonal in both cases thanks to trivial considerations of properties under translation in x , which are unaffected by the 1D mapping. The fact that the basis Eq. (2.32) remains orthogonal, and in particular linearly independent, after restriction to the real axis makes it manifest that the mapping between the original lowest Landau level and its image \mathcal{L}_τ in the 1D Hilbert space is one-to-one.

We note that working with y -guiding-center eigenstates instead of x (as in our initial discussion for the cylinder) leaves the second quantized Hamiltonian invariant, except for the trivial replacement $\tau \rightarrow -1/\tau$ associated with the “modular S transformation”. This is due to the “S-duality” of the physics on the torus (see, e.g., Ref. [54]). The torus Hamiltonian (2.26) was already written with reference to the orbitals (2.32).

2.4.5 Definition of a 2-body operator generating the deformation of guiding center variables

We first explain how to relate a result obtained within the 1D framework introduced above to the desired one, which uses ordinary conventions based on a Hilbert space equipped with the standard 2D scalar product. Fig. 2.4 shows this process in detail. The top segment shows lowest Landau levels $\mathcal{L}_\tau, \mathcal{L}_{\tau'}$ at different modular parameter that, using the 2D to

$$\begin{array}{ccc}
\mathcal{H} & & \mathcal{H} \\
\updownarrow & \text{flow of Eq. (14)} & \updownarrow \\
\mathcal{L}_\tau & \xrightarrow{\quad} & \mathcal{L}_{\tau'} \\
\uparrow I_\tau \cong & & \cong \uparrow I_{\tau'} \\
\tilde{G}_\tau \mathcal{L} & & \mathcal{L} \tilde{G}_{\tau'} \\
\updownarrow c_n^\dagger \rightarrow \mathcal{N}_n(\tau) c_n^\dagger & & \updownarrow c_n^\dagger \rightarrow \mathcal{N}_n(\tau') c_n^\dagger \\
G_\tau \mathcal{L} & \xrightarrow{P e^{\int_\tau^{\tau'} G_\tau d\tau}} & \mathcal{L} G_{\tau'}
\end{array}$$

Figure 2.4: Commuting diagram displaying the various Hilbert spaces and sub-spaces defined in the main text, and operators acting between them.

1D mapping defined in the text, have been embedded into the same larger 1D Hilbert space \mathcal{H} . At the same time, each Landau level is isomorphic (through embeddings $I_\tau, I_{\tau'}$, which will be defined in the following) to the same finite dimensional “abstract” Landau level space \mathcal{L} , in which only the guiding center degrees of freedom are represented. The generator \tilde{G}_τ of changes in the guiding center degrees of freedom with τ is first constructed using the normalization conventions of the 1D Hilbert space. It is related by a similarity transformation to the operator G_τ , which generates the analogous changes for the normalization convention of the usual 2D Hilbert space. In the horizontal direction, we have mappings between states defined for values of the modular parameter. The upper line is defined through the flow of Eq. (2.31), which describes precisely the change of the Laughlin state, restricted to the real axis. The lower line represents the corresponding change in guiding center degrees of freedom, given by Eq. (2.58). The operator G_τ is constructed such that the diagram commutes.

Next we will do the exact process showed in Fig. 2.4 in detail. Suppose we have an

operator \tilde{G}_{τ_x} (\tilde{G}_{τ_y}) that generates the change with τ_x (τ_y) in the coefficients $\tilde{C}_{\{n_k\}}(\tau)$ in the expansion of the Laughlin state,

$$\psi_{1/q}(\tau) = \sum_{\{n_k\}} \tilde{C}_{\{n_k\}}(\tau) \mathcal{A} \tilde{\chi}_{n_1}(z_1, \tau) \cdot \dots \cdot \tilde{\chi}_{n_N}(z_N, \tau), \quad (2.33)$$

where $\tilde{\chi}_n(z, \tau) = \mathcal{N}_n(\tau) \chi_n(z, \tau)$, $\mathcal{N}_n(\tau)$ being the factor that normalizes the state χ_n with respect to the 1D scalar product, ${}_1\langle \phi | \psi \rangle_1 = \int_0^1 dx \phi^*(x) \psi(x)$, i.e., $\mathcal{N}_n = {}_1\langle \chi_n | \chi_n \rangle_1^{-1/2}$, and we will often leave the τ -dependence understood. Likewise, we have dropped the label ℓ for now, which is just a spectator in the “heat equation” (2.31). \mathcal{A} denotes anti-symmetrization in the indices n_k . The Laughlin state in Eq. (2.33) is a member of the subspace \mathcal{L}_τ of \mathcal{H} as defined in the preceding section. We may now map the state (2.33) to the abstract Landau level Hilbert space \mathcal{L} as discussed in Sec. 2.4.1, by applying a projector which “forgets” the degrees of freedom associated with kinetic momenta. This situation is represented by the diagram in Fig. 2.4.

If we perform this projection orthogonally with respect to the 1D scalar product, we obtain a ket

$$|\tilde{\psi}_{1/q}(\tau)\rangle = \sum_{\{n_k\}} \tilde{C}_{\{n_k\}}(\tau) c_{n_1}^\dagger \dots c_{n_N}^\dagger |0\rangle. \quad (2.34)$$

By definition, we then have

$$\nabla_\tau |\tilde{\psi}_{1/q}(\tau)\rangle = \tilde{\mathbf{G}}_\tau |\tilde{\psi}_{1/q}(\tau)\rangle, \quad (2.35)$$

where we assume $\tilde{\mathbf{G}}_\tau = (\tilde{G}_{\tau_x}, \tilde{G}_{\tau_y})$ to be of the form

$$\tilde{\mathbf{G}}_\tau = \sum_{mm'nn'} \mathbf{G}_{mm'nn'} c_m^\dagger c_{m'}^\dagger c_n c_{n'}. \quad (2.36)$$

In the end, one wants to do the projection of Eq. (2.33) orthogonally with respect to the original 2D scalar product. This gives

$$|\psi_{1/q}(\tau)\rangle = \sum_{\{n_k\}} C_{\{n_k\}}(\tau) c_{n_1}^\dagger \dots c_{n_N}^\dagger |0\rangle \quad (2.37)$$

where $C_{\{n_k\}} = \mathcal{N}_{n_1} \dots \mathcal{N}_{n_N} \tilde{C}_{\{n_k\}}$ from the change of normalization, $c_n^\dagger \rightarrow \mathcal{N}_n c_n^\dagger$. This implies the relation

$$|\psi_{1/q}(\tau)\rangle = e^{\sum_{n=0}^{L-1} \ln[\mathcal{N}_n(\tau)] c_n^\dagger c_n} |\tilde{\psi}_{1/q}(\tau)\rangle. \quad (2.38)$$

From this last line, we obtain that the desired operator \mathbf{G}_τ defined by Eq. (2.29) is related to Eq. (2.36) via ⁴

$$\begin{aligned} \mathbf{G}_\tau &= \sum_n \frac{\nabla_\tau \mathcal{N}_n(\tau)}{\mathcal{N}_n(\tau)} c_n^\dagger c_n \\ &+ \sum_{mm'nn'} \frac{\mathcal{N}_m(\tau) \mathcal{N}_{m'}(\tau)}{\mathcal{N}_n(\tau) \mathcal{N}_{n'}(\tau)} \mathbf{G}_{mm'nn'} c_m^\dagger c_{m'}^\dagger c_n c_{n'}. \end{aligned} \quad (2.39)$$

With this we have completely relegated the solution of the problem to the 1D Hilbert space.

We point out that the 1D mapping described above may generally provide an efficient way to calculate the matrix elements of operators acting within the lowest Landau level on the

⁴It turns out that the final form of $\tilde{\mathbf{G}}_\tau$ also contains a one body part that we omit in (2.36), (2.39) for brevity. However this part transforms analogously.

torus.⁵ In this case, Eq. (2.39) will apply without the τ -derivative part. The explicit form of $\mathcal{N}_n(\tau)$ will be given below.

We now define the operator I_τ which injects the ket $|\tilde{\psi}_{1/q}(\tau)\rangle$ into $\mathcal{L}_\tau \in \mathcal{H}$, by sending $c_n^\dagger|0\rangle$ to $\tilde{\chi}_n(\tau)$. Thus

$$\psi_{1/q} = I_\tau|\tilde{\psi}_{1/q}\rangle. \quad (2.40)$$

For the time being, we work at fixed τ_x . Using the heat equation (2.31) with $\partial_\tau = -i\partial_{\tau_y}$ and differentiating Eq. (2.40), one obtains

$$\partial_{\tau_y}\psi_{1/q} = i\Delta\psi_{1/q} = (\partial_{\tau_y}I_\tau)|\tilde{\psi}_{1/q}\rangle + I_\tau\tilde{G}_{\tau_y}|\tilde{\psi}_{1/q}\rangle, \quad (2.41)$$

where Δ denotes the differential operator on the right hand side of Eq. (2.31), and we also used Eq. (2.35).

For $\text{Re } \tau = \text{Re } \tau'$, it is easy to see that $P_\tau\partial_{\tau_y}I_\tau \equiv 0$, where P_τ is the orthogonal projection operator onto \mathcal{L}_τ (we work in the 1D Hilbert space now, and will always refer to its scalar product when not stated otherwise). To see this, it is sufficient to observe that $\langle\chi_m|\partial_{\tau_y}\chi_n\rangle = 0$ for all m, n . This follows from the fact that $\langle\chi_m(\tau)|\chi_n(\tau')\rangle = \delta_{m,n}\langle\chi_m(\tau)|\chi_m(\tau')\rangle$ is always real for $\text{Re } \tau = \text{Re } \tau'$. Thus, acting on the last equation with P_τ , we get

$$P_\tau\Delta P_\tau\psi_{1/q} = P_\tau\Delta P_\tau I_\tau|\psi_{1/q}\rangle = I_\tau\tilde{G}_{\tau_y}|\tilde{\psi}_{1/q}\rangle.$$

where we have also inserted P_τ before $\psi_{1/q} \in \mathcal{L}_\tau$. Since we only care about how the operator \tilde{G}_{τ_y} acts on these q states, for which we have the last equation, we may thus define this

⁵We are indebted to G. Möller for this observation.

operator though the identity

$$\tilde{G}_{\tau_y} = I_\tau^{-1} P_\tau \Delta P_\tau I_\tau. \quad (2.42)$$

The last equation expresses that the matrix elements of \tilde{G}_{τ_y} are just those of the differential operator Δ restricted to the LLL subspace \mathcal{L}_τ . These can thus be calculated straightforwardly by evaluating the standard expression for two-body operators:

$$G_{mm'nn'}^y = \frac{1}{2} \int_0^1 dx \int_0^1 dx' \tilde{\chi}_m^*(x) \tilde{\chi}_{m'}^*(x') \Delta \tilde{\chi}_{n'}(x') \tilde{\chi}_n(x). \quad (2.43)$$

As a last step, we calculate G_{τ_y} by fixing the normalization convention for single particle orbitals in accordance with the usual 2D scalar product, as displayed in Eq. (2.39). We may then obtain the generator for changes in τ_x simply by studying the analytic properties of the coefficients $C_{\{n_k\}}(\tau)$ in Eq. (2.37). As shown in Appendix .1, one has

$$\partial_{\tau_x} C_{\{n_k\}} = -i \partial_{\tau_y} C_{\{n_k\}} + i \frac{N}{4\tau_y}. \quad (2.44)$$

We can thus let $G_{\tau_x} = -i G_{\tau_y} + i \frac{\hat{N}}{4\tau_y}$. Moreover, Eq. (2.44) follows from the fact that $C_{\{n_k\}}/\tau_y^{N/4}$ is holomorphic in τ . We may use this insight to conveniently redefine the normalization of the Laughlin states via

$$\psi_{1/q}^\ell(z_1, \dots, z_N, \tau) = \tau_y^{-N/4} \psi_{1/q}^\ell(z_1, \dots, z_N, \tau). \quad (2.45)$$

The corresponding generator for changes in τ_y is then given by $G'_{\tau_y} = G_{\tau_y} - \frac{\hat{N}}{4\tau_y}$. In the following, we will always refer to the normalization convention (2.45). Dropping all primes,

we then have

$$G_{\tau_x} = -iG_{\tau_y} \equiv G_\tau . \quad (2.46)$$

With the ket $|\psi_{1/q}(\tau)\rangle$ now referring to Eq. (2.45), $|\psi_{1/q}(\tau)\rangle$ is then holomorphic in τ , and we have

$$\partial_\tau |\psi_{1/q}(\tau)\rangle = G_\tau |\psi_{1/q}(\tau)\rangle . \quad (2.47)$$

We present our final result as

$$G_\tau = G_0 + \frac{1}{4\pi i q} G_1 + q G_2 . \quad (2.48)$$

Here, the first term corresponds to $-i$ times the one-body operator in the y -component of Eq. (2.39), plus the shift of $iN/4\tau_y$ shown in Eq. (2.44). Defining the functions

$$\mathcal{S}_n^a = \sum_l (2\pi i[lL + n])^a e^{-2\pi L\tau_y(l+n/L)^2} , \quad (2.49)$$

the normalization factors defined above correspond to $(\mathcal{N}_n)^{-2} = \sqrt{2L/\tau_y} \mathcal{S}_n^0$. We thus get

$$G_0 = \frac{i}{2} \sum_n \frac{\partial_{\tau_y} \mathcal{S}_n^0}{\mathcal{S}_n^0} c_n^\dagger c_n = -\frac{1}{4\pi i L} \sum_n \frac{\mathcal{S}_n^2}{\mathcal{S}_n^0} c_n^\dagger c_n . \quad (2.50)$$

Next, G_1 is the contribution coming from the differential operator ∂_X^2 in Eq. (2.31). Note that after normal ordering, the square of a single body operator still contains a single body operator. We thus get the following result:

$$G_1 = \left(\frac{q}{L}\right)^2 \left[\sum_n \frac{\mathcal{S}_n^2}{\mathcal{S}_n^0} c_n^\dagger c_n + \sum_{n_1 \neq n_2} \frac{\mathcal{S}_{n_1}^1 \mathcal{S}_{n_2}^1}{\mathcal{S}_{n_1}^0 \mathcal{S}_{n_2}^0} c_{n_1}^\dagger c_{n_1} c_{n_2}^\dagger c_{n_2} \right] . \quad (2.51)$$

Note that $\mathcal{S}_n^2 \neq (\mathcal{S}_n^1)^2$, owing to the fact that $P_\tau \partial_X^2 P_\tau \neq (P_\tau \partial_X P_\tau)^2$. Finally, G_2 relates to the θ -function part of Eq. (2.31). Eq. (2.43) can be evaluated by expanding the factors in the integrand, which are all periodic in x, x' , into Fourier series. For the $\partial\theta/\theta$ -terms, this can be done by contour integration and using known properties of θ functions. Key steps in this term are shown in Appendix .3. With the help of Eq. 30, straightforward calculation allows one to express G_2 through rapidly converging, albeit multiple sums,

$$G_2 = \frac{1}{2} \sum_{n_1 n_2 n_3 n_4} \frac{\Delta_{n_1 n_2 n_3 n_4}}{\mathcal{S}_{n_1}^0 \mathcal{S}_{n_2}^0} c_{n_1}^\dagger c_{n_2}^\dagger c_{n_4} c_{n_3} + \frac{1}{2} C \hat{N} (\hat{N} - 1), \quad (2.52)$$

and we have defined the function

$$\begin{aligned} \Delta_{n_1 n_2 n_3 n_4} &= \delta_{n_1+n_2, n_3+n_4} \frac{2\pi}{i} \sum_{\substack{n \neq 0 \\ n = n_3 - n_1 \pmod L}} \left(\frac{e^{i\pi\tau n}}{1 - e^{2i\pi\tau n}} \right)^2 \\ &\sum_{l_1} e^{i\pi\tau L[(n_1+n)/L+l_1]^2} (e^{i\pi\tau L(n_1/L+l_1)^2})^* \\ &\sum_{l_4} (e^{i\pi\tau L[(n_4+n)/L+l_4]^2})^* e^{i\pi\tau L(n_4/L+l_4)^2}, \end{aligned} \quad (2.53)$$

and the (τ -dependent) constant

$$C = \frac{1}{4\pi i} \left[\int_{-1/2}^{1/2} \left(\frac{\partial_\tau \theta_4}{\theta_4} \right)^2 dz - \pi^2 \right]. \quad (2.54)$$

In the above, the Kronecker δ is understood to be periodic, enforcing identity $n_1+n_2 = n_3+n_4 \pmod L$.

2.4.6 Symmetry considerations

The operator G_τ defined in the preceding section is manifestly invariant under magnetic translations in the x -direction. In the basis we chose here, this is tantamount to the conservation, modulo L , of the “center-of-mass” operator $\sum_n n c_n^\dagger c_n$. On the other hand, the operator is not invariant under magnetic translations in the τ -direction, which amounts to an ordinary shift of the orbital indices. As already pointed out in Sec. 2.4.2, the symmetrized operator

$$G_{\tau,\text{sym}} = \frac{1}{L} \sum_{n=0}^{L-1} T_\tau^n G_\tau (T_\tau^\dagger)^n \quad (2.55)$$

also satisfies Eq. (2.29), where T_τ generates magnetic translations in τ . This is a trivial consequence of the fact that the $|\psi_{1/q}^\ell(\tau)\rangle$ transform among themselves under T_τ , and all satisfy Eq. (2.29). Likewise, each term on the right hand side of Eq. (2.55) satisfies Eq. (2.29).

We may thus define the $L - 1$ linearly independent 2-body operators

$$D_n = G_{\tau,\text{sym}} - T_\tau^n G_\tau (T_\tau^\dagger)^n, \quad n = 0 \dots L - 2, \quad (2.56)$$

that all annihilate each of the q -fold degenerate Laughlin states,

$$D_n |\psi_{1/q}^\ell\rangle = 0. \quad (2.57)$$

We note that the D_n are not in any obvious way related to the operators $Q_R^\dagger Q_R$ of the pseudo-potential Hamiltonian, with Q_R given by (2.26). Indeed, the D_n have a non-vanishing single-body term, whereas the $Q_R^\dagger Q_R$ do not. The D_n thus represent a new class of two-body operators that annihilate the torus Laughlin states (in the absence of quasi-holes). For

$q = 3$ and various values of particle number N , we have verified that the property (2.56) characterizes the $q = 3$ Laughlin states uniquely.

Note that the single-body contribution to $G_{\tau, \text{sym}}$ is proportional to the particle number, as explained in Sec. 2.4.2. This term can thus be replaced by a constant when acting on the Laughlin state, and hence can be ignored altogether in practical calculations, where the real part of this constant is usually adjusted to fix the normalization of the state (see below), and the imaginary part only affects the phase convention. For the same reason, we do not need the value of the τ -dependent constant C defined in Eq. (2.54) for the purpose of practical calculations.

2.4.7 Presentation of the Laughlin state through its thin torus limit

In the following, we will generally identify G_τ with the symmetrized operator $G_{\tau, \text{sym}}$ discussed in the preceding section, without carrying along the "sym" label. Putting the results of Sec. 2.4.5 in integral form, we have, via Eq. (2.47),

$$|\psi_{1/q}^\ell(\tau')\rangle = P e^{\int_\tau^{\tau'} G_\tau d\tau} |\psi_{1/q}^\ell(\tau)\rangle, \quad (2.58)$$

where P means path ordering. The integral in Eq. (2.58) should be interpreted as a complex contour integral, where the result is independent of the path connecting τ and τ' . This is so since by construction, G_τ generates exactly the change with τ of the guiding center coordinates of the states in Eq. (2.45), which are single valued functions of τ . (This requires that we carry along all the τ -dependent constant number terms mentioned in the preceding

section.)

We may also want to add, possibly different, real constants to G_{τ_x} and G_{τ_y} , such that the normalization of the Laughlin state is preserved under the evolution with these operators. When evaluating Eq. (2.58) iteratively, this simply corresponds to normalizing the state at each step. We denote the accordingly modified operators by $G_{\tau_x}^N$ and $G_{\tau_y}^N$, and introduce the operator valued 1-form $dG_\tau^N = G_{\tau_x}^N d\tau_x + G_{\tau_y}^N d\tau_y$. We may then write

$$|\psi_{1/q}^\ell(\tau')\rangle_N = P e^{\int_\tau^{\tau'} dG_\tau^N} |\psi_{1/q}^\ell(\tau)\rangle_N, \quad (2.59)$$

where the subscript N denotes normalized Laughlin states. We are now interested in the thin torus limit $\tau \rightarrow i\infty$, in which $|\psi_{1/3}^\ell(\tau)\rangle_N$ approaches the ket $|100100100\dots\rangle$, [55] or one related to the latter through repeated action of T_τ . Here, the labels 100100100... are occupation numbers in the basis (2.32). Given our earlier discussion for the cylinder, it cannot be taken for granted that Eq. (2.59) remains well-defined in this limit. On the other hand, it may seem plausible that this is the case, since the operators $G_{\tau_x}^N$, $G_{\tau_y}^N$ do generate off-diagonal matrix elements when acting on the thin torus state, unlike the case of the cylinder. It thus seems feasible that the full Laughlin states at arbitrary τ admit the following presentation in terms of their respective thin torus limit,

$$|\psi_{1/q}^\ell(\tau)\rangle_N = P e^{\int_\infty^\tau dG_\tau^N} |\dots 100\dots 100\dots 100\dots\dots\rangle, \quad (2.60)$$

where the pattern on the right hand side denotes one of the q thin torus patterns at filling factor $1/q$. The correctness of the above assertion remains non-trivial, however, as the

$\tau' \rightarrow \infty$ limit in Eq. (2.59) must be taken with care. In the next Section we provide numerical evidence for $q = 3$, demonstrating the above relation for various particle numbers N . We thus find that the full torus Laughlin state may be generated from its given thin torus limit via application of the above path-ordered exponential involving the two-body operator constructed here. We conjecture that this is true for general q . An application demonstrating this technique will be discussed in the following.

2.5 Application: Hall viscosity

As an application of our findings in Sec. 2.4, we use Eq. (2.60) (or the differential form Eq. (2.47)) to calculate the $\nu = 1/3$ torus Laughlin state along a contour in the complex τ -plane, starting from the thin torus limit at $\tau = i\infty$. As a physical motivation for calculating the Laughlin state along such contours, we will be asking how the Hall viscosity[48] evolves along such contours. Hall viscosity is “a non dissipative viscosity coefficient analogous to Hall conductivity, for paired states, Laughlin states, and more general quantum Hall states”. It is an invariant within a topological phase. This quantity is naturally related to the main theme of our work, i.e., changes of the Laughlin state with changes in geometry. The notion of a Hall viscosity of fractional quantum Hall liquids has generated much interest recently,[48, 21, 51] expanding earlier work[2] on integer quantum Hall states. In particular, in an insightful paper, [48] Read has derived a general relation between the viscosity of a quantum Hall fluid and a characteristic quantum number \bar{s} , which can be interpreted as “orbital spin per particle” and is related to the conformal field theory description of the state in question. Here we only give a brief summary of the relevant definitions, following closely Ref. [51], to

which we refer the interested reader for details.

We denote the fourth-rank viscosity tensor of the fluid by η_{abcd} , where we are interested in the case of two spatial dimensions. In a situation with no dissipation, only its anti-symmetric or ‘‘Hall viscosity’’ component $\eta_{abcd}^{(A)} = -\eta_{cdab}^{(A)}$ may be non-zero, and this is possible only when time reversal symmetry and the symmetry under reflection of space are both broken. This is the situation in a magnetic field (where in a constant field, only the product of these two symmetries is unbroken).

We now consider a system with periodic boundary conditions defined by two periods $\mathbf{L}_1 = (L_1, 0)$ and $\mathbf{L}_2 = (L_1\tau_x, L_1\tau_y)$, and Hamiltonian

$$H = \frac{1}{2} \sum_{i=1}^N g^{ab} \pi_{ia} \pi_{ib} + P_{\text{LLL}} \sum_{m,n} \sum_{i < j} V(\|x_{ij} + m\mathbf{L}_1 + n\mathbf{L}_2\|_g) P_{\text{LLL}} \quad (2.61)$$

Here, π_a is a component of the kinetic momentum, P_{LLL} denotes LLL-projection, and we have introduced a metric g_{ab} . We have also introduced the ‘‘periodized’’ version of a potential V that depends on x_i, x_j only via $\|x_{ij}\|_g \equiv g_{ab} x_{ij}^a x_{ij}^b$ with $x_{ij} = x_i - x_j$. We follow Ref. [51] and parametrize the metric via $g(\lambda) = \Lambda^T \Lambda$, $\Lambda = \exp(\lambda)$, where Λ can be viewed as a coordinate transformation that transforms the identity metric into the metric g . Clearly, g is invariant under $\Lambda \rightarrow R\Lambda$, where R is a rotation matrix. Since λ can be interpreted as being proportional to an ‘‘infinitesimal version’’ of Λ , whose rotational component is just its anti-symmetric part, we may fix this rotational degree of freedom by requiring λ to be symmetric. Then, the Hall viscosity of the ground state of Eq. (2.61) can be related[2, 51, 9] to the adiabatic curvature on the space of background metrics, here parameterized by the

symmetric matrix λ . Specializing to $g = \text{id}$, we have:

$$\eta_{abcd}^{(A)} = -\frac{1}{V} F_{ab;cd} \quad (2.62)$$

where $F_{ab;cd}$ is the Berry curvature

$$F_{ab;cd} = -2\text{Im}\langle \partial_{\lambda_{ab}}\psi | \partial_{\lambda_{cd}}\psi \rangle|_{g=\text{id}}, \quad (2.63)$$

and ψ denotes the ground state of Eq. (2.61). $F_{ab;cd}$ clearly has the anti-symmetry of $\eta_{abcd}^{(A)}$, and it is also symmetric in the index pairs ab and cd . Furthermore, at least in the thermodynamic limit of large L_1 , one would expect $\eta_{abcd}^{(A)}$ to acquire full rotational symmetry. In two dimensions, this requires the trace $\eta_{abcc}^{(A)}$ to vanish, where we use the sum convention, and similarly for the first index pair. (In higher dimensions, rotational symmetry requires $\eta^{(A)}$ to vanish identically). Moreover, in an incompressible fluid, the strain tensor u_{ab} must be traceless. Therefore, since the viscosity couples to the rate of strain \dot{u}_{ab} via $\eta_{abcd}^{(A)}\dot{u}_{cd}$ to give a viscous contribution to the stress tensor, only the traceless part of $\eta_{abcd}^{(A)}$ is of interest. It therefore makes sense to restrict our attention to traceless λ_{ab} , corresponding to volume preserving coordinate transformations. Requiring $F_{ab;cd}$ thus to be anti-symmetric, symmetric in the first and second pair, as well as traceless, in $D = 2$ the associated curvature 2-form $F = \frac{1}{2}F_{ab;cd} d\lambda_{ab} \wedge d\lambda_{cd}$ can only depend on the following two independent linear combinations of 1-forms, $d\lambda_{11} - d\lambda_{22}$ and $d\lambda_{12} + d\lambda_{21}$. Hence it must be proportional to their product:[51]

$$F = -\frac{1}{2}s (d\lambda_{11} - d\lambda_{22}) \wedge (d\lambda_{12} + d\lambda_{21}), \quad (2.64)$$

and we introduced a proportionality factor $-s/2$ whose physical meaning will be given below.

The above expression in Eq. (2.62) gives

$$\eta_{abcd}^{(A)} = \eta^{(A)} (\delta_{ad}\epsilon_{bc} + \delta_{bc}\epsilon_{ad}) \quad (2.65)$$

with

$$\eta^{(A)} = \frac{1}{2} \bar{s} \bar{n} \hbar, \quad (2.66)$$

where $\bar{n} = N/V$ is the particle density, $\bar{s} = s/N$, and we have restored a factor of \hbar . As shown in Ref. [48], in the thermodynamic limit the parameter \bar{s} is quantized and can be identified with the average orbital spin per particle, which is related to the conformal dimension of the field describing particles in the conformal field theory description of the state. It is further related to the topological shift on the sphere, \mathcal{S} , of the underlying state via $\bar{s} = \mathcal{S}/2$. For the Laughlin 1/3 state, $\bar{s} = 3/2$.

We now consider fixed boundary conditions described by τ , and introduce a metric that corresponds to the infinitesimal transformation

$$d\lambda = \frac{1}{2\tau_y} \begin{pmatrix} -d\tau_y & d\tau_x \\ d\tau_x & d\tau_y \end{pmatrix}. \quad (2.67)$$

It is not difficult to see that the corresponding metric change is equivalent to changing the modular parameter τ to $\tau' = \tau + d\tau_x + id\tau_y$. We may thus rewrite Eq. (2.64) as

$$F = -\frac{N\bar{s}}{2\tau_y^2} d\tau_x \wedge d\tau_y. \quad (2.68)$$

To each λ can be associated a τ' , where $\Lambda = \exp(\lambda)$ is the coordinate transformation that changes the τ -boundary condition into a τ' -boundary condition, where

$$\tau' = \frac{\Lambda \mathbf{L}_1 \cdot \Lambda \mathbf{L}_2 + i \Lambda \mathbf{L}_1 \times \Lambda \mathbf{L}_2}{\|\Lambda \mathbf{L}_1\|^2}. \quad (2.69)$$

For fixed τ , we now parameterize λ , and thus the metric, by τ' . (Note that the right hand side of Eq. (2.69) can be viewed as a function of Λ and τ .) Eq. (2.68) then implies that

$$\bar{s} = \frac{4\tau_y^2}{N} \text{Im} \langle \partial_{\tau'_x} \psi | \partial_{\tau'_y} \psi \rangle. \quad (2.70)$$

We emphasize that in the above, $\psi \equiv \psi(\tau, g_\tau(\tau'))$ always satisfies the same boundary condition defined by τ , and depends on τ' only through the metric. At the same time, $\psi(\tau, g_\tau(\tau'))$ is related to $\psi(\tau', \text{id})$ by the unitary transformation $\chi_n(\tau, g_\tau(\tau')) \rightarrow \chi_n(\tau', \text{id})$, with $\chi_n(\tau, g(\tau'))$ the deformed version of the state (2.32) in the presence of the metric $g(\tau')$. However, for fixed τ , the $\psi(\tau, g_\tau(\tau'))$ live in the same Hilbert space,[51] independent of τ' . The advantage of introducing both τ and τ' , where the former describes boundary conditions, and the latter describes the “true geometry” of the system, is that we may restrict ourselves to metrics $g_\tau(\tau')$ in the vicinity of the identity (corresponding to τ' close to τ), such that Eq. (2.62) is directly applicable.

We now consider $\psi = \psi_{1/3}^N$, the normalized Laughlin 1/3 state (where we suppress labels τ , τ' , and ℓ). We have the expansion

$$\psi_{1/3}^N = \sum_{\{n_k\}} C_{\{n_k\}}^N(\tau') |\{n_k\}\rangle_g, \quad (2.71)$$

and $|\{n_k\}_g\rangle$ is short for the Slater determinant $\mathcal{A} [\chi_{n_1}(z_1, \tau, g(\tau')) \cdots \chi_{n_N}(z_N, \tau, g(\tau'))]$.

We write $-2\text{Im} \langle \partial_{\tau'_x} \psi | \partial_{\tau'_y} \psi \rangle = \nabla_{\tau'} \times A$ where

$$A = i \sum_{\{n_k\}} (|C_{\{n_k\}}^N|^2 {}_g \langle \{n_k\} | \nabla_{\tau'} | \{n_k\} \rangle_g + C_{\{n_k\}}^{N*} \nabla_{\tau'} C_{\{n_k\}}^N) \quad (2.72)$$

is the Berry connection. It turns out that in the first term, which describes the change of the LLL basis with τ' , ${}_g \langle \{n_k\} | \nabla_{\tau'} | \{n_k\} \rangle_g$ is independent of $\{n_k\}$, and contributes a constant 1/2 to Eq. (2.70).[34] The second term depends on the changes of the $C_{\{n_k\}}$ with τ' , which we described in the preceding section. We first assume the general situation where this change is described by Eq. (2.29) with two generators G_{τ_x} and G_{τ_y} that are not necessarily related and that do not necessarily preserve the normalization of the state. It is straightforward to show that the contribution from the second term then leads to the following connected expectation value,

$$\begin{aligned} & -2 \text{Im} \sum_{\{n_k\}} \partial_{\tau'_x} C_{\{n_k\}}^{N*} \partial_{\tau'_y} C_{\{n_k\}}^N \\ & = i \left[\langle G_{\tau_x}^\dagger G_{\tau_y} - G_{\tau_y}^\dagger G_{\tau_x} \rangle - \langle G_{\tau_x}^\dagger \rangle \langle G_{\tau_y} \rangle + \langle G_{\tau_y}^\dagger \rangle \langle G_{\tau_x} \rangle \right], \end{aligned} \quad (2.73)$$

where expectation values on the right hand side are taken in the state Eq. (2.71). The last two terms take care of the normalization, and will cancel if both operators are anti-Hermitian (describing unitary evolution), in which case the expression reduces to the expectation value of a commutator. Note also that the expression is invariant under constant shifts of any of the two operators. We now specialize to the case where these operators are related by

Eq. (2.46). Plugging Eq. (2.72), Eq. (2.73) into Eq. (2.70), this gives

$$\bar{s} = \frac{1}{2} + \frac{4\tau_y^2}{N} |\Delta G_\tau|^2, \quad (2.74)$$

where $|\Delta G_\tau| = (\langle G_\tau^\dagger G_\tau \rangle - \langle G_\tau^\dagger \rangle \langle G_\tau \rangle)^{1/2}$ is the variance of the operator G_τ in the state $\psi_{1/3}^N$, and is manifestly positive (the Laughlin state at τ certainly being no eigenstate of G_τ for any τ). As stated above, for the Laughlin state \bar{s} is expected to approach 3/2 in the thermodynamic limit. This has been checked in Ref. [51], by calculating torus Laughlin (and other) states by exact diagonalization of parent Hamiltonians, and computing the Berry curvature by taking overlaps between such states for different τ (or λ). Here we will consider the same problem both as a demonstration and a consistency check of the results presented in the preceding section. To this end, we calculate the Laughlin state from the presentation (2.60), or by numerically integrating the differential equation (2.47) with thin torus initial conditions, and then computing \bar{s} from Eq. (2.74). Note that both steps of the calculation make use of the two-body operator G_τ . In particular, our results will confirm the accuracy of Eq. (2.60), which may be written more carefully as

$$|\psi_{1/q}^\ell(\tau)\rangle_N = \lim_{\tau' \rightarrow i\infty} P e^{\int_{\tau'}^{\tau} dG_\tau^N} |\dots 100\dots 100\dots 100\dots\dots\rangle. \quad (2.75)$$

Evaluating the expression on the right for some large but finite τ' is equivalent to integrating Eq. (2.47) (and normalizing the result), where the thin torus limiting state defines the initial condition at τ' . This obviously introduces some error compared to the full Laughlin state at the initial value τ' , hence also at the final value τ . Since it is not clear a priori how this error

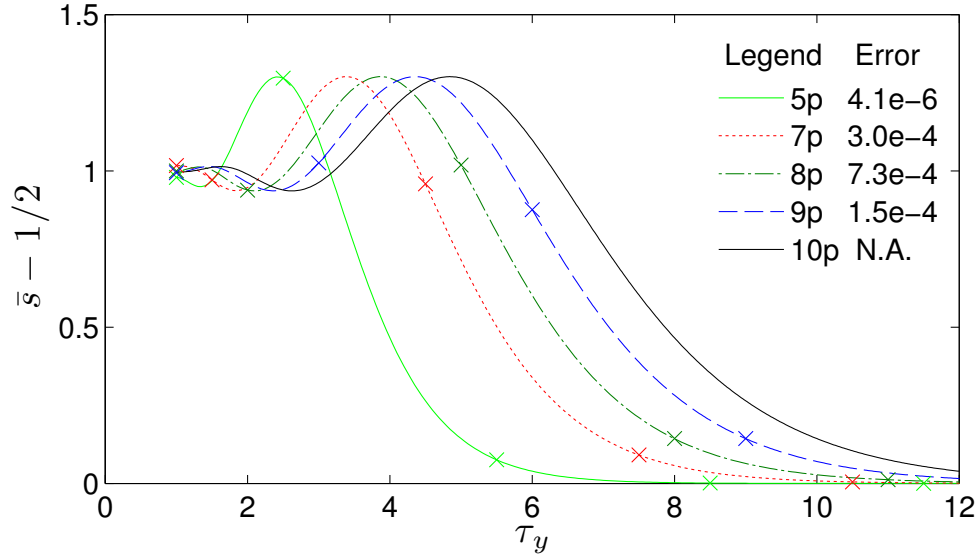


Figure 2.5: Average “orbital spin per particle” \bar{s} as calculated from Eq. (2.70), for the $\nu = 1/3$ torus Laughlin state at τ generated via Eq. (2.75), using the procedure described in the main text.

behaves in the limit of large imaginary τ' , possible pitfalls are that the limit in Eq. (2.75) is ill-defined, or that it is well-defined but does not agree with the Laughlin state.⁶ Our results, however, give strong support of Eq. (2.75).

Fig. 2.5 shows the results for the value of $\bar{s} - 1/2$ from this method for $q = 3$. Beginning with the thin torus state $|100100100\dots\rangle$ at large imaginary τ' , we evolve the state down to $\tau = i$, i.e., a torus of aspect ratio 1, integrating Eq. (2.47) using the classical 4th order Runge-Kutta method. We normalize the state at each step. Final state errors compared with exact diagonalization at $\tau = i$ are shown in Fig. 2.5 for 5 particles for $\tau' = 30i$ and step size $d\tau = 0.01i$, 7 and 8 particles for $\tau' = 30i$ and $d\tau = 0.05i$, 9 particles for $\tau' = 40i$, $d\tau = 0.025i$. 10 particles data is shown for $\tau' = 80i$, $d\tau = 0.02i$. Crosses denote the value of $\bar{s} - 1/2$ obtained from the exactly diagonalized Laughlin state in Eq. (2.70), for comparison.

⁶The latter case is obviously realized for the Laughlin state on the cylinder and the operator G_{r-2} defined in Sec. 2.4.1, where the expression analogous to the right hand side Eq. (2.75) leaves the thin torus limiting state invariant.

The errors of \bar{s} are at or smaller than 10^{-6} in these cases.

For particle numbers $N = 5$ to $N = 9$, we have observed that the error of the state obtained at $\tau = i$, compared to the Laughlin state generated from exact diagonalization of the V_1 Haldane pseudopotential, $|\psi - \psi_{ed}|$, becomes systematically smaller with increasing initial τ' and decreasing step size $d\tau$. The observed state error at $\tau = i$ has been on the order of 10^{-6} for $N = 5$, and on the order of 10^{-4} for $N = 9$. For $N = 10$, we show data based on our method only. Generally, larger N requires larger τ' for the same accuracy.

One can also see from Fig. 2.5 that the expected value of $\bar{s} - 1/2 = 1$ is always approached rather closely for $\tau = i$, though it deviates from this value for $|\tau|$ noticeably larger than 1. The crossover where notable deviations from 1 set in is pushed to larger $|\tau|$ with increased particle number, as expected. However, the value of \bar{s} is found to be much more constant, and close to its expected thermodynamic limit, when instead of varying the modulus of τ we vary its phase at $|\tau| = 1$, even for five particles, as shown in Fig. 2.6.

The state has been evolved out of the thin torus limit first down to $\tau = i$ as described in the caption of Fig. 2.5, and then to $\tau = e^{i\theta}$ using the same method. The step sizes used are $d\theta = 0.01rad$ for 5 particles and $d\theta = 0.001rad$ for 8 and 10 particles. The state difference with the exactly diagonalized Laughlin state at the last step is listed in the figure. $\bar{s} - 1/2$ remains close to 1, as expected in the thermodynamic limit[48], for a wide range of angles θ . These observations are consistent with exact diagonalization data in Ref. [51] for $N = 10$ and (at $\tau = \exp(i\pi/3)$) larger particle number.

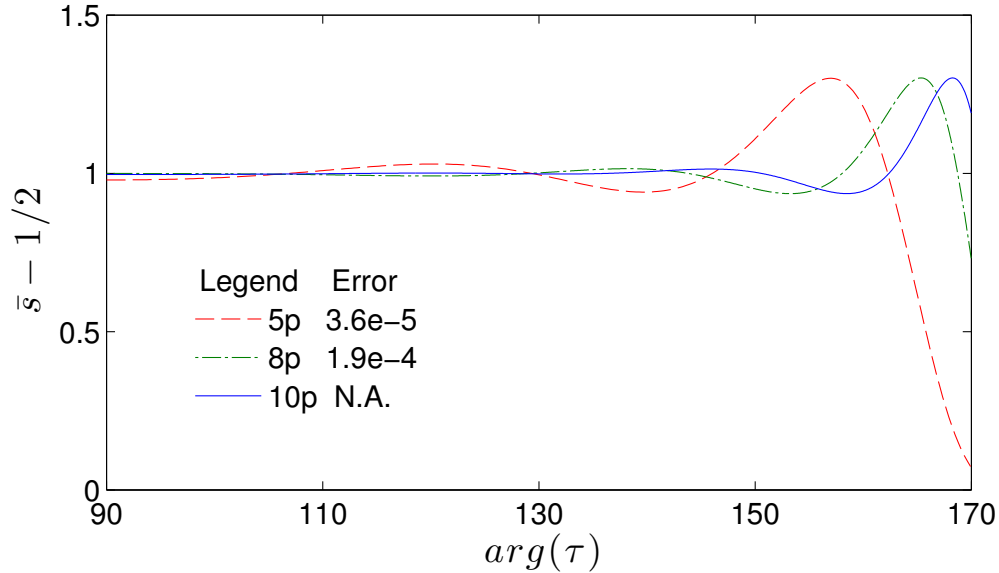


Figure 2.6: Average orbital spin per particle \bar{s} , calculated from Eq. (2.70), for the $\nu = 1/3$ torus Laughlin state, with τ goes along unit circle.

2.6 Discussion

In the preceding sections, we considered the change in the guiding center variables, with modular parameter τ for the torus Laughlin states. Within a given Landau level, the guiding center coordinates fully specify the state. We have shown that this change is generated by a two-body operator G_τ , which we have explicitly constructed. We have demonstrated numerically that by means of this two-body operator, the Laughlin state for any modular parameter τ can be generated from its simple thin torus ($\tau = i\infty$) limit. The ability to generate the full torus Laughlin state in this way may be compared to squeezing rules that follow from the Jack polynomial structure of this state in other geometries.[7, 6] From a practical point of view, however, our method still requires integration of a first order differential equation. While this requires some compromise between accuracy and computational effort, the added benefit is that in the process of the calculation, the Laughlin state is generated

along an entire contour in the complex τ plane, rather than just for a single value of τ . It is thus likely that whenever a moderate error can be tolerated, but many τ values are of interest, our method may become competitive compared to numerical diagonalization. As a demonstration of these features, we have produced results relating to the Hall viscosity that are similar to those of Ref. [51] (and are expected to be identical within numerical accuracy for identical particle number, which we have not yet studied). The Hall viscosity is itself deeply related to our main theme of study, i.e., geometric changes in the Laughlin state,[2, 48, 51] and we have discussed its precise relation to the generator constructed here (Eq. (2.74)), following Ref. [51].

We note that one key ingredient of our procedure is to embed different torus Laughlin states, which are related to one another by the application of strain, into the same Hilbert space. For this we make use of a dimensional reduction that is made possible by the analytic properties of lowest Landau level wave functions on the torus. We argued that this mapping may be useful in other contexts. However, recent work on Hall viscosity[51] achieves the same embedding by a different method, which is to introduce a metric describing the effect of strain, rather than a change in boundary conditions. We conjecture that if we had used this method in Sec. 2.4, we would have directly obtained the symmetrized version of our operator G_τ . In this way, however, we would not have obtained the family of two-body operators given in Sec. 2.4.6, whose members annihilate the torus Laughlin states.

While primarily, we have been working in a finite dimensional Hilbert space that represents guiding center-coordinates only, the operator defined in Sec. 2.4 also naturally acts within the full Hilbert space, which can be viewed as the tensor product of the degrees of freedom for the guiding centers and the dynamical momenta, respectively. Within this larger,

physical, Hilbert space, the operator G_τ generates the change in guiding center degrees of freedom associated to a change in the torus geometry, but not the corresponding change of the Landau level. As pointed out recently by Haldane,[22] the Laughlin state may be generalized by the introduction of a geometric parameter that describes the deformation of guiding center variables in response to a change in the “interaction metric”. The so deformed Laughlin state is still the exact ground state of an appropriately deformed Hamiltonian. The operator that we have constructed can thus also be viewed as generating the change of the torus Laughlin state in response to a change of the interaction metric, i.e., the change in ground state for the corresponding family of deformed pseudo-potential Hamiltonians. For the disc geometry, this problem has been addressed from different angles previously.[51, 47]

We conjecture that the observations made here are not limited to Laughlin states, but can be generalized to other quantum Hall states as well. Indeed, a great wealth of model wave functions is obtained from conformal blocks in rational conformal field theories.[41] For conformal blocks on the torus, the dependence on the modular parameter τ can be described by Knizhnik-Zamolodchikov-Bernard (KZB) type equations.[5] We expect therefore that our approach can be generalized to other trial wave functions related to conformal field theories. The details of such generalizations are left for future work.

Chapter 3

Geometric phase of d-wave vortices in a model of lattice fermions

3.1 Introduction and motivation

In this chapter, we switch our research topic from quantum Hall systems to superconducting systems. The Berry phases usually don't play a dominant role in superconductivity. However, as we have seen in chapter 1, the nature way to introduce Berry phase is applying magnetic field. This is in particularly the case in type II superconductors, where magnetic vortices are allowed to penetrate the superconductor when external magnetic field is applied. A type II superconductor has 2 critical magnetic field H_{c1} and H_{c2} . Below H_{c1} , the whole bulk is superconducting. When the fields exceeds H_{c1} , an Abrikosov lattice of vortices is formed due to the free energy flip of superconducting-normal interface. Inside the vortex, magnetic field penetrates the superconducting layer. When the magnetic field keeps increasing, the Abrikosov lattice become more and more dense. Eventually, the superconductivity

disappears when H_{c2} is reached.

Here we are studying the Berry phase in the parameter space expanded by position of magnetic vortices. The following part of this chapter has been published in Ref. [78].

3.2 Background

Our model description is based on a phenomenology of a BCS-like pairing state with d -wave symmetry, which has led to considerable success in understanding the properties of quasi-particles in high- T_c superconducting cuprates. This includes the mixed state of these systems, where a magnetic field $H_{c1} < H < H_{c2}$ is applied and leads to the presence of an Abrikosov vortex lattice. Effective models[71, 16, 35, 64, 65, 67, 36, 37, 38, 66, 39, 68, 69, 60, 45, 44] have been developed that describe the dynamics of the quasi-particles under the simultaneous influence of magnetic field, the supercurrent flow due to the vortices, and in some cases the underlying microscopic lattice. The vortices of the mixed state are usually assumed to be static, i.e., frozen into the Abrikosov lattice. However, it has been argued[43] that both as a result of the small coherence length ξ , and possibly the proximity to an insulating state, fluctuations of vortices may play a fundamental role. Moreover, at sufficiently high magnetic fields below H_{c2} , it has been predicted that thermal and/or quantum fluctuations may melt the vortex lattice or glass, leading to a “vortex liquid” regime[27]. For all these reasons, it is desirable to construct effective theories that include the vortices as fundamental dynamical degrees of freedom. [40] Such a construction is readily available in systems where the constituent particles are bosons, through the well-known Kramers-Wannier duality [13]. In Fermi systems, however, the vortex degrees of freedom

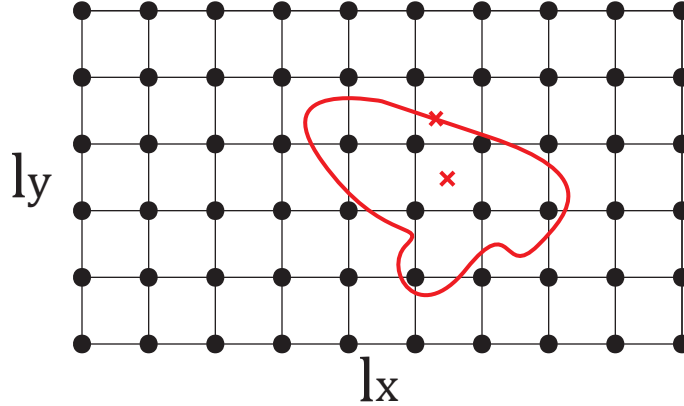


Figure 3.1: A magnetic unit cell of fermionic lattice for d -wave superconductor with 2 vortices embedding. The ground state gain Berry phase when one vortex goes around a close loop.

only exist as dual partners of bosonic Cooper pairs that are themselves emergent particles. This arguably complicates the task of passing directly from a microscopic description in terms of electrons to an effective theory in terms of vortices, requiring more ad hoc assumptions. Such effective theories have been previously discussed in a continuum formalism.[43] In this chapter, we aim to establish some key parameters of these theories in a microscopic lattice model. This is similar in spirit, but physically different, from earlier considerations for bosons in the absence of a lattice[25]. These defining parameters include the quantum curvature felt by the vortices in the condensate, that is, the effective magnetic field, or Berry curvature, experienced by them, and their mutual statistics. Specifically in the d -wave pairing case, where the continuum description of vortices is somewhat plagued by subtleties concerning self-adjoint extensions[37], our microscopic starting point also serves as lattice regularization[64], which allows for a controlled study of the desired universal properties.

3.3 Model description

We will study the Berry phases[8] of vortices in the *BCS-Hofstadter* model on a square lattice in Fig. 3.1, which has been used previously as a microscopic description of the mixed state in the cuprates[65].

$$H = \sum_{\langle \mathbf{r}\mathbf{r}' \rangle} [-t_{\mathbf{r}\mathbf{r}'} c_{\mathbf{r}\sigma}^\dagger c_{\mathbf{r}'\sigma'} + \frac{\Delta_{\mathbf{r}\mathbf{r}'}}{2} (c_{\mathbf{r}\downarrow}^\dagger c_{\mathbf{r}'\uparrow}^\dagger + c_{\mathbf{r}'\downarrow}^\dagger c_{\mathbf{r}\uparrow}^\dagger) + h.c.] - \mu N \quad (3.1)$$

In the above, \mathbf{r} is the lattice site coordinate shown as black dots in Fig. 3.1. The sum $\langle \mathbf{r}\mathbf{r}' \rangle$ is over the nearest neighbors, and the hopping terms are just those of the Hofstadter model, to be described below. The corresponding uniform magnetic flux through the plaquettes of the lattice mirrors the fact that the penetration depth is much larger than the coherence length, as befits a type II superconductor. Assuming symmetric gauge $\mathbf{A}(\mathbf{r}) = (-y/2, x/2)\Phi$, where Φ the magnetic flux per plaquette, the hopping amplitude assumes the form

$$t_{\mathbf{r}\mathbf{r}'} = t e^{-i \int_{\mathbf{r}}^{\mathbf{r}'} \mathbf{A} \cdot d\mathbf{l}}, \quad (3.2)$$

where \mathbf{r} refers to the discrete sites of the lattice. The d-wave pairing term is defined as

$$\Delta_{\mathbf{r}\mathbf{r}'} = \eta_{\mathbf{r}-\mathbf{r}'} \Delta_{0,\mathbf{r}\mathbf{r}'} e^{i\theta_{\mathbf{r}\mathbf{r}'}} \quad (3.3)$$

$$\eta_{\mathbf{r}-\mathbf{r}'} = +/- \text{ if } (\mathbf{r} - \mathbf{r}') \parallel \hat{\mathbf{x}}/\hat{\mathbf{y}} \quad (3.4)$$

Here, $\eta_{\mathbf{r}-\mathbf{r}'}$ encodes the d-wave symmetry. $\Delta_{0,\mathbf{r}\mathbf{r}'}$ is essentially constant, except for a suppression of amplitude near the vortex core. We follow Ref. [67] in defining the pairing phase

factor $e^{\theta_{\mathbf{r}\mathbf{r}'}}$ via

$$e^{i\theta_{\mathbf{r}\mathbf{r}'}} \equiv \frac{e^{i\phi(\mathbf{r})} + e^{i\phi(\mathbf{r}')}}{|e^{i\phi(\mathbf{r})} + e^{i\phi(\mathbf{r}')}|}, \quad (3.5)$$

i.e., as a link-centered average of a field $\phi(r)$ that satisfies the following continuum equations,

$$\nabla \times \nabla \phi(\mathbf{r}) = 2\pi \hat{z} \sum_i \delta(\mathbf{r} - \mathbf{r}_i) \quad (3.6a)$$

$$\nabla \cdot \nabla \phi(\mathbf{r}) = \mathbf{0}, \quad (3.6b)$$

where the \mathbf{r}_i denote the vortex positions, shown as the red crosses in Fig. 3.1 which can take on continuous values. The total number of vortices n_V is equal to the number of half flux-quanta Φ_0 , $l_x l_y \Phi = n_V \Phi_0$ where $\Phi_0 = \pi$ in natural units, and l_x, l_y are the number of unit cells in the x and y direction, respectively. Eq. (3.6) can be solved[38] via

$$\phi(\mathbf{r}) = \sum_i \{arg[\sigma(z - z_i, \omega, \omega')]\} + 2\gamma(x - x_i)(y - y_i) + \mathbf{v}_0 \cdot \mathbf{r}, \quad (3.7)$$

where $\sigma(z, \omega, \omega')$ is the Weierstrass sigma-function with half periods $\omega = l_x/2$, $\omega' = il_y/2$, $z = x + iy$, and the sum is over vortex positions. Integration constants $\mathbf{v}_0 = 2 \sum_i \mathbf{A}(\mathbf{r}_i)$ and $\gamma = \frac{\pi}{2l_x l_y} - \frac{\eta}{l_x}$ have been chosen such that the superfluid velocity $\mathbf{v}_S = \nabla \phi/2 - \mathbf{A}$ satisfies periodic boundary conditions, and averages to zero over the magnetic unit cell[67], and $\eta = \zeta(\omega)$ is pure imaginary, with ζ the Weierstrass zeta-function. This field $\phi(r)$ has a self consistent topological feature. It has 2π winding around the magnetic vortices. This feature remains to the pairing phase factor by Eq. (3.5). We made a brief plot of superfluid

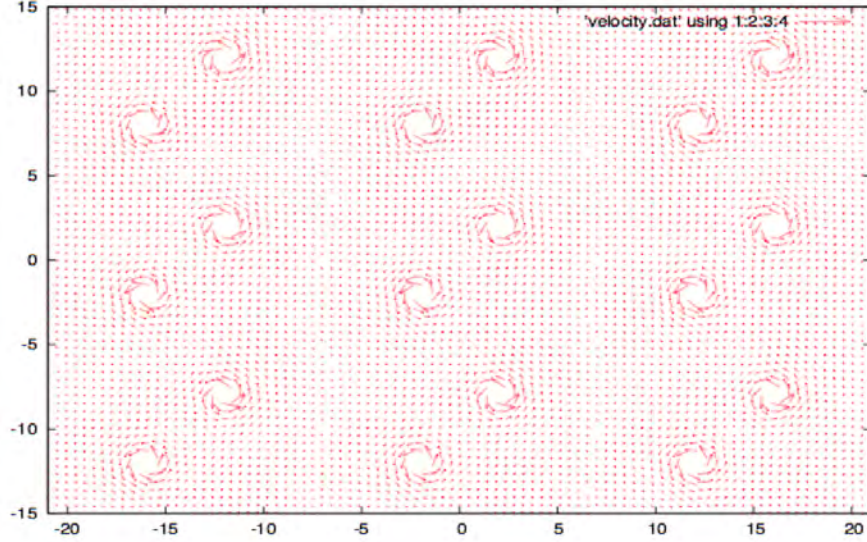


Figure 3.2: Superfluid velocity in a 7 by 5 magnetic unit cell. The positions of vortices are (2,2) and (-2,-2).

velocity for two vortices in a 7 by 5 magnetic unit cell in Fig. 3.2. It is easy to see that the velocity is periodic in l_x and l_y as it should be. The model retains the main feature of d-wave superconductor vortex.

The pairing phase factor $e^{i\theta_{\mathbf{r}\mathbf{r}'}}$ in Eq.(3.5) is ill-defined when the denominator goes to 0. This is unacceptable since we mean to continuously change vortex coordinates in the following. To remove this singularity, we define $\Delta_{0,\mathbf{r}\mathbf{r}'}$ as

$$\Delta_{0,\mathbf{r}\mathbf{r}'} \equiv \Delta_0 \left[1 - \exp\left(-\frac{|e^{i\phi(\mathbf{r})} + e^{i\phi(\mathbf{r}')}|}{\xi}\right) \right] \quad (3.8)$$

where Δ_0 and ξ are constant parameters. This leads to a suppression of pairing amplitude on links near the vortex, hence ξ may be thought of as a core radius.

We further impose periodic magnetic boundary conditions on our model as follows:

$$c_{\mathbf{r}} = T_x^{l_x} c_{\mathbf{r}} (T_x^\dagger)^{l_x} = T_y^{l_y} c_{\mathbf{r}} (T_y^\dagger)^{l_y} \quad (3.9)$$

$$T_{\mathbf{R}} c_{\mathbf{r}} T_{\mathbf{R}}^\dagger = c_{\mathbf{r}+\mathbf{R}} e^{i \int_{\mathbf{r}}^{\mathbf{r}+\mathbf{R}} \mathbf{A} \cdot d\mathbf{l} + i \mathbf{R} \times \mathbf{r} \Phi} \quad (3.10)$$

In the above, the magnetic translation operators T_x and T_y are defined by letting $\mathbf{R} = \hat{x}$ or \hat{y} . We note that with the boundary conditions (3.9) imposed on electron operators, the physics is also periodic in the vortex positions \mathbf{r}_i . That is, one may see that the formal replacements $\mathbf{r}_i \rightarrow \mathbf{r}_i + l_x \hat{x}$, $\mathbf{r}_i \rightarrow \mathbf{r}_i + l_y \hat{y}$ affect the Hamiltonian by a unitary transformation, as given explicitly below. In particular, the quasi-particle spectrum is invariant under such replacements.

3.4 Calculation of the Berry phase

In the following, we will consider the model Eqs. (3.1)-(3.9) as a function of vortex positions $\{\mathbf{r}_i\}$. We note that the simultaneous presence of the magnetic field and the discrete ionic lattice generically opens up a gap in the quasi-particle spectrum of the d -wave superconductor, except for special vortex configurations that respect inversion symmetry [66]. The Berry phase associated with the motion of vortices is thus well-defined. We further remark that the model defined above is traditionally studied by means of a singular gauge transformation [16], that, on average, removes the magnetic field. This is inconvenient for present purposes, since the precise transformation depends on vortex positions, and the Berry phase is clearly not invariant under unitary transformations that vary along the particular path in question.

We thus need to stay within the present framework of magnetic translations and associated boundary conditions.

To study the Berry phases associated with the motion of vortices, we first note that within our model the vortex positions are well-defined continuous parameters that are, at least for large enough lattice, entirely encoded in the pairing amplitudes $\Delta_{\mathbf{r}\mathbf{r}'}$. The Berry phase associated with vortex motion along closed paths may be computed via

$$e^{i\gamma} \approx \langle \Omega_1 | \Omega_m \rangle \cdots \langle \Omega_3 | \Omega_2 \rangle \cdot \langle \Omega_2 | \Omega_1 \rangle, \quad (3.11)$$

where the $|\Omega_i\rangle$ are the ground states of the system along a reasonably fine discretization of the path. The above formula has the advantage (over the standard integral formula) that a random, discontinuous phase that each $|\Omega_i\rangle$ acquires in numerical diagonalization automatically cancels. Each ground state is constructed as the vacuum of Bogoliubov operators

$$\gamma_{n\uparrow} = \sum_{\mathbf{r}} (u_n^*(\mathbf{r})c_{\mathbf{r}\uparrow} - v_n^*(\mathbf{r})c_{\mathbf{r}\downarrow}^\dagger) \quad (3.12)$$

$$\gamma_{n\downarrow} = \sum_{\mathbf{r}} (u_n^*(\mathbf{r})c_{\mathbf{r}\downarrow} + v_n^*(\mathbf{r})c_{\mathbf{r}\uparrow}^\dagger) \quad (3.13)$$

where the matrices $U_{\mathbf{r}n} = u_n(\mathbf{r})$, $V_{\mathbf{r}n} = v_n(\mathbf{r})$, satisfy Bogoliubov-deGennes equations

$$\begin{pmatrix} -t - \mu & -\Delta \\ -\Delta^* & t^* + \mu \end{pmatrix} \begin{pmatrix} U \\ -V \end{pmatrix} = E_n \begin{pmatrix} U \\ -V \end{pmatrix} \quad (3.14)$$

for non-negative eigenvalues E_n . It is clear from Eq. (3.12) that the state $|\tilde{0}\rangle = \prod_{\mathbf{r}} c_{\mathbf{r}\downarrow}^\dagger |0\rangle$ is a vacuum of both the operators $\gamma_{n\uparrow}$ and $\gamma_{n\downarrow}^\dagger$, where $|0\rangle$ is the vacuum of the $c_{\mathbf{r}\sigma}$ operators.

The ground state of the Hamiltonian thus can be constructed as

$$|\Omega\rangle = \prod_n \gamma_{n\downarrow} |\tilde{0}\rangle. \quad (3.15)$$

Using this last relation, and the inverse of Eq. (3.12), one readily obtains

$$\langle \Omega_i | \Omega_j \rangle = \det(U_i U_j^\dagger + V_i V_j^\dagger). \quad (3.16)$$

3.5 Results

We first consider the important special case of Eq. (3.1) with $\mu = 0$, or half-filling. In this case the Hamiltonian is invariant under the *anti*-unitary charge conjugation operator defined via $\mathcal{C} c_{\mathbf{r}\sigma} \mathcal{C} = (-1)^{\mathbf{r}} c_{\mathbf{r}\sigma}^\dagger$, and the unique ground state $|\Omega\rangle$ is then invariant under \mathcal{C} as well (up to a phase that can be made trivial). It then follows directly from Eq. (3.11) that $e^{i\gamma} = \pm 1$. The first immediate conclusion from this is that as long as vortices are moved along contractible paths, the Berry phase must be +1 for continuity reasons. If vortices were hard-core particles this would, in principle, still leave the possibility of fermionic statistics. However, careful examination shows that the Hamiltonian can be analytically continued without difficulty into configurations where two vortices fuse into a double vortex at a given location. Exchange paths are thus contractible, and hence vortices must satisfy bosonic statistics. We have tested this for various lattice sizes and exchange paths. The model does, however, become singular when vortex positions are formally approaching lattice sites, see Eq. (3.7). It is thus possible that lattice sites carry an effective π -flux felt by vortices

encircling such sites. We have carefully checked that this is not the case in our model. Hence at half filling, all Berry phases are unity. The above observations also hold for the s -wave case.

The observation that vortices are bosonic is non-trivial, since time reversal symmetry is absent, and hence generically in two spatial dimensions even non-Abelian statistics are possible, as is the case if the pairing symmetry is $p+ip$ [28]. Indeed, when we move away from half filling, there is no longer any symmetry that requires the Berry phase to be trivial. We will now show that this situation leads to a very intricate landscape of non-trivial quantum curvature.

The Berry curvature is defined as the Berry phase around an infinitesimal area, divided by the size of this area. In the following, we consider a lattice containing only two vortices in the presence of periodic boundary condition. As Fig. 3.1 shows, One vortex remains fixed, while for any point within the unit cell, we calculate the Berry curvature associated with the motion of the other vortex according to Eq. (3.11). The Berry phase around arbitrary loops can be obtained as the integral of the Berry curvature over the enclosed area. The result for a 12×10 lattice at $\mu = 0.05$ is presented in Fig. 3.3(a). It is apparent that the Berry curvature in this model is a highly non-trivial function of position for any $\mu \neq 0$. One observes that the curvature is conspicuously concentrated on the links and the sites of the lattice, even though the vortex positions themselves are formally not tied to the discrete lattice. Singular structures form in particular around the lattice sites. The remaining space within the plaquettes is nearly flat. These are described by $B(\mathbf{r}) \sim a_i \delta(\mathbf{r} - \mathbf{r}_i) + f_i(\theta)/r$, where $B(\mathbf{r})$ is the curvature, and θ, r refer to polar coordinates with the lattice site \mathbf{r}_i at the origin. The parameters a_i and the functions f_i depend sensitively on details such as

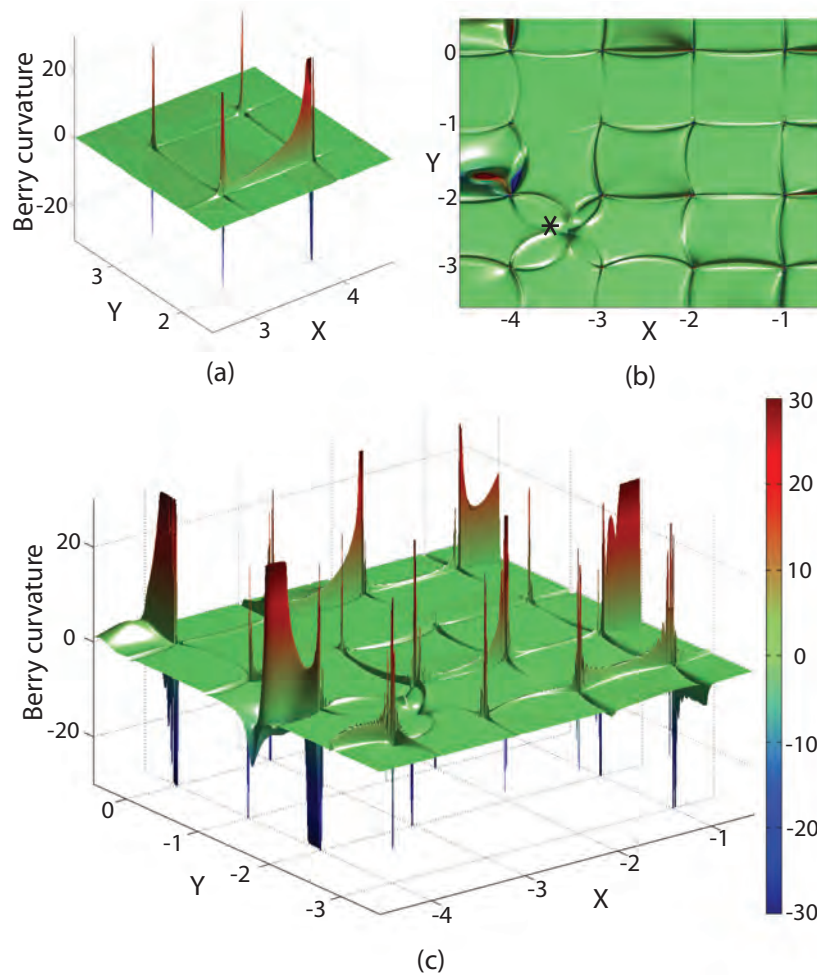


Figure 3.3: Berry curvature for 12 by 10 lattice in the presence of two vortices, for $\mu = 0.05$. (a): 3D view of the Berry curvature in the vicinity of one plaquette. (b) Top view of the lattice. (c): 3D view of the entire lattice.

the lattice size, μ , the site index i , and the position of the other, fixed vortex. Yet another interesting feature in Fig. 3.3(b) is the structure seen in the vicinity of the fixed vortex, which is somewhat reminiscent of the shape of a $d_{x^2-y^2}$ orbital. However, this structure does not seem to be reflective of by the pairing symmetry, but rather more the lattice symmetry, as similar calculations for the s-wave case show. We note that again no singularity indicative of a flux tube carried by the fixed vortex appears in Fig. 3.3(b) at the position of this vortex labeled by asterisk. This implies that we should still think of these vortices as bosons, which move in an effective background magnetic field.

The complex nature of these features and the strong sensitivity on model parameters are likely yet another facet of the fractal nature of the physics of the Hofstadter model. To wit, in view of the fractal nature of the wave-vector dependence of spectral features of the Hofstadter model, it is reasonable to expect that the response to a spatially inhomogeneous perturbation (coupling to many different wave vectors) is characterized by complicated and possibly chaotic spatial modulations. The addition of a pairing order parameter with vortices clearly represents such a perturbation. Here we are mostly interested in how to reconcile the complex features seen at $\mu \neq 0$ with the trivial ones seen at $\mu = 0$. It is clear that our ability to precisely define the vortex position on scales below the lattice constant is dependent on conventions, even though in the present case a natural convention is available, since our ground states are naturally parameterized by the vortex positions in the continuum field (3.6) used to define the Hamiltonian. We have, however, tested the robustness of the qualitative features shown in Fig. 3.3 by varying the precise form of the pairing order parameter Eq. (3.3). In particular, we have varied the core parameter ξ in Eq. (3.8), and tested various alternative forms for Eq. (3.5). We also introduced variations in the boundary conditions described

above. In all cases we found that the qualitative features of the Berry curvature remained unaltered. Although we believe that the curvature landscape of Fig. 3.3(c) is interesting in its own right, it is appropriate to make this landscape subject to some coarse graining procedure. It is interesting to ask whether such coarse graining leads to a recovery of one of the basic facts suggested by conventional wisdom about vortex-boson duality, namely that the curvature discussed above is directly tied to particle (here, Cooper-pair) density. We will show in the following that this statement is recovered when the Berry curvature is averaged over the magnetic unit cell (as opposed to the, typically much smaller, lattice unit cell). To this end, we again consider a lattice containing only two vortices within a single magnetic unit cell, subject to the boundary conditions (3.9).

Let the coordinates of the “moving” vortex be $\mathbf{r} = (x, y)$. As remarked initially, a formal shift of x by l_x changes the Hamiltonian by a gauge transformation. We have $H \rightarrow U_x^\dagger H U_x$ with $U_x = e^{i\pi(1-y/l_y)\hat{N}/2}$, where \hat{N} is the particle number operator. Analogous relations hold for $y \rightarrow y + l_y$, with $U_y = e^{i\pi(1+x/l_x)\hat{N}/2}$. We now calculate the Berry phase associated with a rectangular path of dimensions l_x, l_y around the lattice. We may then choose a ground state phase convention $|\Omega(\mathbf{r})\rangle$ along the path satisfying

$$\begin{aligned} |\Omega(\mathbf{r} + l_y \hat{y})\rangle &= U_y^\dagger |\Omega(\mathbf{r})\rangle \\ |\Omega(\mathbf{r} + l_x \hat{x})\rangle &= U_x^\dagger |\Omega(\mathbf{r})\rangle \end{aligned} \tag{3.17}$$

along the horizontal and vertical path segments, respectively. The consistency of Eq. (3.17) with the continuity of $|\Omega(\mathbf{r})\rangle$ along the path follows from the observation that for any ground state, $U_y^\dagger U_x^\dagger U_y U_x |\Omega\rangle = |\Omega\rangle$. The latter holds because $U_y^\dagger U_x^\dagger U_y U_x = \exp(i\pi\hat{N})$ and because

the ground state Eq. (3.15) always has even particle number parity. We determine the Berry phase for the rectangular path as the integral over the Berry connection, $\langle \Omega(\mathbf{r}) | \nabla | \Omega(\mathbf{r}) \rangle$, where we observe that

$$\begin{aligned} \langle \Omega(\mathbf{r} + l_x \hat{x}) | \nabla | \Omega(\mathbf{r} + l_x \hat{x}) \rangle &= \langle \Omega(\mathbf{r}) | U_x \nabla U_x^\dagger | \Omega(\mathbf{r}) \rangle \\ &= \langle \Omega(\mathbf{r}) | \nabla | \Omega(\mathbf{r}) \rangle + \frac{i\pi}{2l_y} \langle \hat{N} \rangle \hat{y}. \end{aligned} \quad (3.18)$$

It is clear that only the last term survives a cancellation between the vertical path segments, giving $i\pi \langle \hat{N} \rangle / 2$. The same contribution is obtained from the horizontal segment. We thus obtain $\gamma = \pi \langle \hat{N} \rangle$, or 2π times the number of Cooper pairs in the system, in agreement with general expectations based on duality arguments applied to Cooper pairs[43]. It is worth noting that the quantity γ , when expressed as an integral of the Berry curvature over the entire lattice, is formally reminiscent of a Chern number. It is not truly a Chern number, though, since the boundary conditions (3.17) do not quite allow one to make contact with one-dimensional vector bundles over the torus. Indeed, γ is not quantized, as $\langle \hat{N} \rangle$ may take on arbitrary values in $[0, 2l_x l_y]$. We note that the derivation above is independent of the pairing symmetry.

3.6 Discussion

The present study establishes several aspects of Berry phases associated with vortex motion in a microscopic model of superconducting lattice fermions. It is shown that these vortices behave as bosons which, away from half filling, are subject to a non-trivial effective magnetic field. In an average sense, it has been shown that this effective field is tied to the density of

Cooper pairs. This is expected based on boson-vortex duality, and was seen to emerge here in a microscopic model of fermions. We emphasize that the simple relation between Cooper-pair density and effective field is only seen to emerge after averaging over a magnetic unit cell. This may be used to justify a direct proportionality between Cooper pair density and Berry curvature in the long wavelength effective theory. However, our results also indicate that care must be used in order to justify such a relationship in general. On the one hand, this is true because of the relatively large non-uniformity of the observed Berry curvature within the magnetic unit cell. Moreover, in the presence of particle hole symmetry we have found that the Berry phase associated with closed paths is always zero, and thus corresponds to π times the average enclosed particle number only for such paths that happen to enclose an even number of lattice sites. In this case, the background field appearing in the effective theory should clearly be zero, and should not follow the total Cooper pair density. This result will be robust to small perturbations respecting particle hole symmetry, and is thus true for a wide class of microscopic models. We conjecture that the complex landscape of the Berry curvature away from half filling is a facet of the fractal properties of the Hofstadter model, and believe that it is worthy of further investigation.

Chapter 4

Summary

It is widely convinced that Berry phase provide additional insight into various quantum systems. In this thesis we take this geometric idea and find it extremely valuable, leading to new understandings in both FQH system and superconducting system.

In the first part of the thesis, we have shown that geometric changes in the guiding center coordinates of the torus Laughlin state are generated by a two-body operator. We have demonstrated that the equation that governs the evolution of the torus Laughlin state as a function of the modular parameter τ can be continued into the thin torus limit. This gives rise to a new presentation of the torus Laughlin state in its second quantized, or guiding center, form. This presentation allows one to calculate the torus Laughlin states in terms of a simple thin torus or “dominance” pattern by means of integration of the flow generated by the two-body operator defined in this work. This operator hence realizes the adiabatic evolution of the simple thin torus product state into the full Laughlin state on regular tori. To demonstrate this, we have numerically compared both the Laughlin state generated from this method, as well as the Hall viscosity derived from it, to exact diagonalization results.

While the demonstration of our new presentation of the torus Laughlin state rests in part on numerics, we will leave more detailed analytic studies for future investigation.

The second part of the thesis deals with Berry phase in a lattice model of d-wave superconductor. The Berry phase of the vortex position shows rich features. Berry curvature is mainly concentrated on the sites and the links of lattice, where electrons are most probably located. We showed bosonic statistics for magnetic vortex for both half filling and way-from-half filling cases, in the sense that there are no singularity of Berry curvature at the site of another vortex. We also find that, average over magnetic unit cell, the Berry phase is proportional to the density of particle numbers. This shares the same expectation of boson-vortex duality, given our system is made of fermions. The duality shall not be taken for granted in our case, because it is the emergent quasiparticles, the cooper pairs, fits into the duality picture.

Appendices

.1 Analytic properties of Laughlin state coefficients

Here is an appendix for connections of derivative of τ_x and τ_y due to analytic continuity of Laughlin state and the single particle LLL orbitals.

For definiteness, we will refer to the Laughlin state $\psi_{1/q}^\ell$ using the normalization conventions (2.23), (2.24). The coefficients $C_{\{n_k\}}(\tau)$ defined in Eq. (2.37) then imply the following expansion of the analytic Laughlin state,

$$\psi_{1/q}^\ell(\tau) = \sum_{\{n_k\}} C_{\{n_k\}}(\tau) \mathcal{A} \chi_{n_1}(z_1, \tau) \cdots \chi_{n_N}(z_N, \tau). \quad (1)$$

Here, as before, the symbol \mathcal{A} denotes anti-symmetrization, and single particle orbitals χ_n are defined in Eq. (2.32). We define new orbitals $\chi'_n(\tau) = \tau_y^{1/4} \chi_n(\tau)$ that are holomorphic in τ , as is the Laughlin state $\psi_{1/q}^\ell(\tau)$. Hence, by acting with $\partial_{\bar{\tau}} = \frac{1}{2}(\partial_{\tau_x} + i\partial_{\tau_y})$ on Eq. (1), we obtain

$$0 = \sum_{\{n_k\}} [\partial_{\bar{\tau}} (C_{\{n_k\}}(\tau)/\tau_y^{N/4})] \mathcal{A} \chi'_{n_1}(z_1, \tau) \cdots \chi'_{n_N}(z_N, \tau). \quad (2)$$

The linear independence of the orbitals $\chi'_n(\tau)$ and of the associated many-particle Slater determinants then implies

$$\partial_{\bar{\tau}} (C_{\{n_k\}}(\tau)/\tau_y^{N/4}) = 0, \quad (3)$$

i.e., the quantities $C_{\{n_k\}}(\tau)/\tau_y^{N/4}$ are holomorphic in τ . Eq. (2.44) follows immediately from Eq. (3).

.2 Hilbert space reduction by magnetic translational operator

Due to the magnetic translational invariance, the Hilbert space of Laughlin state can be reduced by a factor of q . Which will greatly reduce the computation cost of exact diagonalization. We'll briefly discuss how we implemented it in the computation.

First, let's remind how the magnetic translation act on the LLL orbitals χ_l .

$$T_1\chi_l(z) = \chi_l(z + \frac{1}{L}) = e^{2\pi i \frac{l}{L}} \chi_l(z), \quad (4)$$

$$T_2\chi_l(z) = e^{-2\pi i x} \chi_l(z - \frac{\tau}{L}) \propto \chi_{l-1}(z). \quad (5)$$

The Laughlin state has the following magnetic translational property,

$$T_1|\psi_{1/q}^l\rangle = e^{2\pi i(\frac{l}{q} + \frac{L-q}{2q})} |\psi_{1/q}^l\rangle, \quad (6)$$

$$T_2|\psi_{1/q}^l\rangle = e^{i\pi(n-1)} |\psi_{1/q}^l\rangle. \quad (7)$$

where $n = L/q$ is the number of electrons in the Laughlin state.

On the other hand, if the Laughlin state is written in linear combination of multiple particle states.

$$T_1|\psi_{1/q}^l\rangle = e^{2\pi i \sum_m l_m / N} |\psi_{1/q}^l\rangle \quad (8)$$

We can get: $n(l + \frac{L-q}{2}) = \sum_m l_m \pmod{N}$, where l_m is the orbital index for single particle

LLL. It is only true if every term in the Laughlin state has the same center of mass of the guiding center. In other word, the Laughlin state has a fixed center of mass.

We know that the Laughlin State is q -fold degenerated. The degenerated states have different center of mass. We can fix a momentum $k = \sum_m l_m$, to tell which exact state we are in.

$$(T_2)^q |\psi_{1/q}\rangle = e^{i\pi(n-1)q} |\psi_{1/q}\rangle = e^{2\pi ik/n} |\psi_{1/q}\rangle \quad (9)$$

The first equity is from the magnetic translation of Laughlin state, while the later equity is from the conclusion of center of mass we got by applying T_1 .

We can group the multi-particle state components in the Laughlin State by the translation of $(T_2)^q$. In other word, we can symmetrize the state. The symmetrized basis is:

$$|\phi_j^{Symm}\rangle = \frac{\sqrt{L_j}}{n} \sum_{m=1}^n [e^{-2\pi i k m/n} (T_2^q)^m] |\phi_{l_1, \dots, l_n}\rangle \quad (10)$$

Where L_j is the number of states linked by the symmetry operators. Then the Laughlin State is the linear combination of the symmetrized basis.

$$|\psi_{1/q}\rangle = \sum_j A_j |\phi_j^{Symm}\rangle \quad (11)$$

We can see $T_{\hat{y}}^q |\phi_{l_1, \dots, l_n}^{Symm}\rangle = e^{2\pi i k/n} |\phi_{l_1, \dots, l_n}^{Symm}\rangle$, which insure the magnetic translational property of Laughlin states.

If the operator \hat{O} commute with the translational operator $[\hat{O}, T_2^q] = 0$, then \hat{O} is living

in the symmetrized space. (e.g. the V_1 pseudo potential Hamiltonian.)

$$\begin{aligned}\hat{O}|\phi_j^{Symm}\rangle &= \frac{\sqrt{L_j}}{n} \sum_m e^{-2\pi i k m/n} \hat{O}(T_2^q)^m |\phi_{l_1, \dots, l_n}\rangle \\ &= \sum_{m'} B_{m'} |\phi_{m'}^{Symm}\rangle\end{aligned}\tag{12}$$

.3 Evaluation of second quantization of theta-function term in the generator

In this section we will go through the key steps leading to the second quantization of $\partial\theta/\theta$ terms in the generator. We restate the definition of theta function used in the main text.

$$\theta \begin{bmatrix} a \\ b \end{bmatrix} (z, \tau) = \sum_m e^{i\pi\tau(m+a)^2 + 2i\pi(m+a)(z+b)}\tag{13}$$

It is related to the traditional definition of theta function as follows,

$$\theta_1(z, \tau) = \theta \begin{bmatrix} 1/2 \\ 1/2 \end{bmatrix} (z, \tau), \quad \theta_1(0) = 0,\tag{14}$$

$$\theta_4(z, \tau) = \theta \begin{bmatrix} 0 \\ 1/2 \end{bmatrix} (z, \tau), \quad \theta_4\left(\frac{\tau}{2}\right) = 0.\tag{15}$$

From the definition of θ function, We'll write down the periodicity of theta function

explicitly,

$$\theta \begin{bmatrix} a \\ b \end{bmatrix} (z + \tau) = \theta \begin{bmatrix} a \\ b \end{bmatrix} (z) \exp[-i\pi\tau - 2\pi i(z + b)], \quad (16)$$

$$\frac{\theta'(z + \tau)}{\theta(z + \tau)} = -2\pi i + \frac{\theta'(z)}{\theta(z)}, \quad (17)$$

$$\frac{\theta'(z + 1)}{\theta(z + 1)} = \frac{\theta'(z)}{\theta(z)}. \quad (18)$$

If we do a lauren expansion at $z = \tau/2$,

$$\frac{\theta'_4(z)}{\theta_4(z)} = (z - \frac{\tau}{2})^{-1} - i\pi + \dots, \quad (19)$$

then the Cauchy's integral over $(-1/2, 0), (1/2, 0), (1/2, \tau), (-1/2, \tau)$ square loop is

$$\oint \frac{\theta'_4(z)}{\theta_4(z)} e^{2\pi i n z} dz = 2\pi i q^n \quad (20)$$

where $q = e^{i\pi\tau}$, n is arbitrary integer. Note here q is not the inverse of filling factor in Laughlin state. Assume the odd Fourier expansion,

$$\frac{\theta'_4(z)}{\theta_4(z)} = \sum_{n \neq 0} B_n e^{-2\pi i n z} \quad (21)$$

the left side of the Cauchy's integral can be evaluated as follow,

$$(1 - q^{2n}) \int_{-1/2}^{1/2} \frac{\theta'_4(z)}{\theta_4(z)} e^{2\pi i n z} dz = 2\pi i q^n, \quad (22)$$

$$B_n = 2\pi i \frac{q^n}{1 - q^{2n}}. \quad (23)$$

Here we comes,

$$\frac{\theta'_4(z)}{\theta_4(z)} = 2\pi i \sum_{n \neq 0} \frac{q^n}{1 - q^{2n}} e^{-2\pi i n z} \quad (24)$$

Following the same strategy, we assume an even form,

$$\left(\frac{\theta'_4(z)}{\theta_4(z)}\right)^2 = \sum_{n \neq 0} C_n e^{-2\pi i n z} + C_0 \quad (25)$$

Evaluating the Cauchy's integral ($n \neq 0$), we can calculate the coefficients C_n .

$$(1 - q^{2n})C_n + 4\pi i q^{2n} \int_{-1/2}^{1/2} \frac{\theta'_4(z)}{\theta_4(z)} e^{2\pi i n z} dz = 2\pi i (-2\pi i + 2\pi i n) q^n \quad (26)$$

$$C_n = 4\pi^2 \frac{q^n}{1 - q^{2n}} \left(\frac{2q^{2n}}{1 - q^{2n}} - n + 1 \right) \quad (27)$$

Inserting Eq. 24 and 25 into the following expression,

$$\frac{\theta'_1(z)}{\theta_1(z)} = \frac{\theta'_4(z - \tau/2)}{\theta_4(z - \tau/2)} - i\pi \quad (28)$$

$$\frac{\partial_\tau \theta_1(z, \tau)}{\theta_1(z)} = \frac{1}{4\pi i} \frac{\partial_z^2 \theta_1(z)}{\theta_1(z)} = \frac{1}{4\pi i} \left[\left(\frac{\theta'_1(z)}{\theta_1(z)} \right)^2 + \left(\frac{\theta'_1(z)}{\theta_1(z)} \right)' \right] \quad (29)$$

We can get the final equation we desire,

$$\frac{\partial_\tau \theta_1(z, \tau)}{\theta_1(z, \tau)} = \frac{1}{4\pi i} \left[\sum_{n \neq 0} 8\pi^2 \left(\frac{q^n}{1 - q^{2n}} \right)^2 e^{2\pi i n z} + \int_{-1/2}^{1/2} \left(\frac{\theta'_4}{\theta_4} \right)^2 dz - \pi^2 \right] \quad (30)$$

Eq. 30 goes directly into G_2 calculation.

.4 Optimization of the generator in thin limit

Here is some estimation used in the computation process of the generator G_τ . With this, our computation should work even when τ_y very small.

The main difficulties of evaluating the generator is from the G_2 part. We'll discuss the evaluation of $delta$ and $Delta$ function defined below within a certain tolerance tol . again here $q = e^{i\pi\tau}$ is not the inverse of filling factor. The $delta$ part can be easily handled by solving the inequality as follows,

$$delta(l, n) = \sum_{n_1} q^{L[(l+n)/L+n_1]^2} (q^{L(l/L+n_1)^2})^*, \quad (31)$$

$$|q^{L[(l+n)/L+n_1]^2} (q^{L(l/L+n_1)^2})^*| \geq tol, \quad (32)$$

$$-\frac{l+n/2}{L} - \sqrt{\frac{\ln(tol)}{-2\pi L\tau_y} - \frac{n^2}{4L^2}} \leq n_1 \leq -\frac{l+n/2}{L} + \sqrt{\frac{\ln(tol)}{-2\pi N\tau_y} - \frac{n^2}{4L^2}}. \quad (33)$$

It is clear that we only need to sum over a few n_1 terms to get the accurate value of $delta$ function.

In order to estimate $Delta$ function, we may first use the inequalities as follows,

$$\sum_n e^{-an^2} < \frac{2}{\sqrt{a}} \left(1 + \frac{1}{e} + \frac{1}{e^2} + \dots\right) = \frac{2e}{\sqrt{a}(e-1)}. \quad (34)$$

Then the absolute value of $delta$ function has up limit:

$$|delta(l, n)| < e^{-\pi\tau_y \frac{n^2}{2L}} \frac{2e}{\sqrt{2\pi L\tau_y}(e-1)}. \quad (35)$$

The other part of the *Delta* function also has up limit,

$$|\operatorname{csch}(x + iy)| \leq |\operatorname{csch}(x)|, \quad (36)$$

$$|\operatorname{csch}(i\pi n\tau)|^2 \leq \operatorname{csch}^2(\pi n\tau_y). \quad (37)$$

Altogether, the summation terms of Delta function has the following up limit,

$$|\Delta(l_1, l_2, l_4)| = \left| \sum_{n \neq 0} \operatorname{csch}^2(i\pi n\tau) [\delta(l_1, n) \delta(l_4, n)^*] \right| \quad (38)$$

$$\leq \sum_{n \neq 0} \operatorname{csch}^2(\pi n\tau_y) e^{-\pi\tau_y \frac{n^2}{L}} \frac{2e^2}{\pi L\tau_y (e-1)^2}. \quad (39)$$

It is obvious that term inside the summation is a monotonic function when n goes away from 0. So we can compare every term in the summation with the desired tolerance, starting from $n = \pm 1$ to both sides. Once Eq. 39 is smaller than the tolerance, we have already arrived an accurate value of *Delta* function.

Despite of the effectiveness of evaluating the above functions. Care must also be taken when the denominator in the generator goes beyond the minimal value of double precision. By going to thin torus limit, the generator has only 2-body term from G_1 component.

$$\lim_{\tau \rightarrow i\infty} G_\tau = -4\pi L^2 \sum_{n_1 \neq n_2} x_1 x_2 \hat{n}_1 \hat{n}_2, \quad (40)$$

where x_i is the guiding center coordinates,

$$\begin{aligned} x_i &= n_i/L - \text{floor}(n_i/L + 0.5) \quad \text{if } n_i \neq L/2 \\ &= 0 \quad \text{if } n_i = L/2. \end{aligned} \tag{41}$$

With the same argument of symmetrizing with magnetic translation symmetry in the main text, one can get a symmetrized version of the thin limit generator, which uniquely define the dominant thin torus pattern as it's eigenstate with biggest eigenvalue.

Bibliography

- [1] Y. Aharonov and D. Bohm. Significance of electromagnetic potentials in the quantum theory. *Physical Review*, 115(3):485–491, August 1959.
- [2] J. E. Avron, R. Seiler, and P. G. Zograf. Viscosity of quantum hall fluids. *Physical Review Letters*, 75(4):697–700, July 1995.
- [3] E. J. Bergholtz and A. Karlhede. Half-Filled Lowest Landau Level on a Thin Torus. *Physical Review Letters*, 94:26802, 2005.
- [4] E. J. Bergholtz and A. Karlhede. ‘One-dimensional’ theory of the quantum Hall system. *J. Stat. Mech.*, L04001, 2006.
- [5] Denis Bernard. On the wess-zumino-witten models on the torus. *Nuclear Physics B*, 303(1):77–93, June 1988.
- [6] B. Andrei Bernevig and F. D. M. Haldane. Generalized clustering conditions of jack polynomials at negative jack parameter α . *Physical Review B*, 77:184502, May 2008.
- [7] B. Andrei Bernevig and F. D. M. Haldane. Model fractional quantum hall states and jack polynomials. *Physical Review Letters*, 100(24):246802, June 2008.
- [8] M. V. Berry. Quantal phase factors accompanying adiabatic changes. *Proceedings of the Royal Society of London. A. Mathematical and Physical Sciences*, 392(1802):45–57, March 1984.
- [9] Barry Bradlyn, Moshe Goldstein, and N. Read. Kubo formulas for viscosity: Hall viscosity, ward identities, and the relation with conductivity. *Physical Review B*, 86(24):245309, December 2012.
- [10] Shiing-shen Chern. Characteristic classes of hermitian manifolds. *Annals of Mathematics*, 47(1):85–121, January 1946. ArticleType: research-article / Full publication date: Jan., 1946 / Copyright 1946 Annals of Mathematics.
- [11] P. a. M. Dirac. Quantised singularities in the electromagnetic field. *Proceedings of the Royal Society of London. Series A*, 133(821):60–72, September 1931.
- [12] G. Fano, F. Ortolani, and E. Colombo. Configuration-interaction calculations on the fractional quantum hall effect. *Physical Review B*, 34(4):2670–2680, August 1986.
- [13] Matthew P. A. Fisher and D. H. Lee. Correspondence between two-dimensional bosons and a bulk superconductor in a magnetic field. *Phys. Rev. B*, 39:2756–2759, Feb 1989.

- [14] John Flavin and Alexander Seidel. Abelian and non-abelian statistics in the coherent state representation. *Physical Review X*, 1:021015, Dec 2011.
- [15] John Flavin, Ronny Thomale, and Alexander Seidel. Gaffnian holonomy through the coherent state method. *Physical Review B*, 86:125316, Sep 2012.
- [16] M. Franz and Z. Tešanović. Quasiparticles in the vortex lattice of unconventional superconductors: Bloch waves or landau levels? *Phys. Rev. Lett.*, 84(3):554, January 2000.
- [17] Liang Fu and C. L. Kane. Topological insulators with inversion symmetry. *Phys. Rev. B*, 76:045302, Jul 2007.
- [18] Martin Greiter, Xiao-Gang Wen, and Frank Wilczek. Paired hall state at half filling. *Physical Review Letters*, 66(24):3205–3208, June 1991.
- [19] F. D. M. Haldane. Fractional quantization of the hall effect: A hierarchy of incompressible quantum fluid states. *Physical Review Letters*, 51(7):605–608, August 1983.
- [20] F. D. M. Haldane. Model for a quantum hall effect without landau levels: Condensed-matter realization of the "parity anomaly". *Phys. Rev. Lett.*, 61:2015–2018, Oct 1988.
- [21] F. D. M. Haldane. "hall viscosity" and intrinsic metric of incompressible fractional hall fluids. *arXiv:0906.1854*, June 2009.
- [22] F. D. M. Haldane. Geometrical description of the fractional quantum hall effect. *Physical Review Letters*, 107(11):116801, September 2011.
- [23] F. D. M. Haldane and E. H. Rezayi. Periodic Laughlin-Jastrow wave functions for the fractional quantized hall effect. *Physical Review B*, 31:2529–2531, Feb 1985.
- [24] F. D. M. Haldane and E. H. Rezayi. Spin-singlet wave function for the half-integral quantum hall effect. *Physical Review Letters*, 60:956–959, Mar 1988.
- [25] F. D. M. Haldane and Yong-Shi Wu. Quantum dynamics and statistics of vortices in two-dimensional superfluids. *Phys. Rev. Lett.*, 55:2887–2890, Dec 1985.
- [26] B.I. Halperin. Theory of the quantized hall conductance. *Helvetica Physica Acta*, 56:75–102, 1983.
- [27] David A. Huse, Matthew P. A. Fisher, and Daniel S. Fisher. Are superconductors really superconducting? *Nature*, 358(6387):553–559, 1992.
- [28] D. A. Ivanov. Non-Abelian statistics of Half-Quantum vortices in p-Wave superconductors. *Phys. Rev. Lett.*, 86(2):268, January 2001.
- [29] J. K. Jain. Composite-fermion approach for the fractional quantum hall effect. *Phys. Rev. Lett.*, 63:199–202, Jul 1989.

- [30] K. v. Klitzing, G. Dorda, and M. Pepper. New method for high-accuracy determination of the fine-structure constant based on quantized hall resistance. *Phys. Rev. Lett.*, 45:494–497, Aug 1980.
- [31] R. B. Laughlin. Quantized hall conductivity in two dimensions. *Physical Review B*, 23(10):5632–5633, May 1981.
- [32] R. B. Laughlin. Anomalous quantum hall effect: An incompressible quantum fluid with fractionally charged excitations. *Physical Review Letters*, 50(18):1395–1398, May 1983.
- [33] Dung-Hai Lee and Jon Magne Leinaas. Mott insulators without symmetry breaking. *Phys. Rev. Lett.*, 92:096401, Mar 2004.
- [34] Péter Lévy. Berry phases for landau hamiltonians on deformed tori. *Journal of Mathematical Physics*, 36(6):2792–2802, June 1995.
- [35] Luca Marinelli, B. I. Halperin, and S. H. Simon. Quasiparticle spectrum of d-wave superconductors in the mixed state. *Phys. Rev. B*, 62(5):3488, 2000.
- [36] Ashot Melikyan and Zlatko Tešanović. Model of phase fluctuations in a lattice d-wave superconductor: Application to the cooper-pair charge-density wave in underdoped cuprates. *Phys. Rev. B*, 71(21):214511, June 2005.
- [37] Ashot Melikyan and Zlatko Tešanović. Mixed state of a lattice d-wave superconductor. *Phys. Rev. B*, 74(14):144501, October 2006.
- [38] Ashot Melikyan and Zlatko Tešanović. Dirac-Bogoliubov-deGennes quasiparticles in a vortex lattice. *Phys. Rev. B*, 76(9):094509, 2007.
- [39] Ashot Melikyan and Oskar Vafek. Quantum oscillations in the mixed state of d-wave superconductors. *Phys. Rev. B*, 78(2):020502, July 2008.
- [40] Ari Mizel. Quantum vortex dynamics from the microscopic hamiltonian. *Phys. Rev. B*, 73(17):174502, May 2006.
- [41] Gregory Moore and Nicholas Read. Nonabelions in the fractional quantum hall effect. *Nuclear Physics B*, 360(23):362–396, August 1991.
- [42] Masaaki Nakamura, Zheng-Yuan Wang, and Emil J. Bergholtz. Exactly solvable fermion chain describing a $=1/3$ fractional quantum hall state. *Physical Review Letters*, 109(1):016401, July 2012.
- [43] Predrag Nikolić and Subir Sachdev. Effective action for vortex dynamics in clean d-wave superconductors. *Phys. Rev. B*, 73(13):134511, April 2006.
- [44] Predrag Nikolić, Subir Sachdev, and Lorenz Bartosch. Electronic states near a quantum fluctuating point vortex in a d-wave superconductor: Dirac fermion theory. *Phys. Rev. B*, 74(14):144516, October 2006.

- [45] Predrag Nikoli and Subir Sachdev. Low energy theory of a single vortex and electronic quasiparticles in a d-wave superconductor. *Physica C: Superconductivity*, 460462, Part 1(0):256 – 260, 2007.
- [46] Xiao-Liang Qi. Generic wave-function description of fractional quantum anomalous hall states and fractional topological insulators. *Physical Review Letters*, 107(12):126803, September 2011.
- [47] R.-Z. Qiu, F. D. M. Haldane, Xin Wan, Kun Yang, and Su Yi. Model anisotropic quantum hall states. *Physical Review B*, 85(11):115308, March 2012.
- [48] N. Read. Non-abelian adiabatic statistics and hall viscosity in quantum hall states and p_x+ip_y paired superfluids. *Physical Review B*, 79(4):045308, January 2009.
- [49] N. Read and E. Rezayi. Quasiholes and fermionic zero modes of paired fractional quantum hall states: The mechanism for non-abelian statistics. *Physical Review B*, 54(23):16864–16887, December 1996.
- [50] N. Read and E. Rezayi. Beyond paired quantum hall states: Parafermions and incompressible states in the first excited landau level. *Physical Review B*, 59(12):8084–8092, March 1999.
- [51] N. Read and E. H. Rezayi. Hall viscosity, orbital spin, and geometry: Paired superfluids and quantum hall systems. *Physical Review B*, 84(8):085316, August 2011.
- [52] E. H. Rezayi and F. D. M. Haldane. Laughlin state on stretched and squeezed cylinders and edge excitations in the quantum hall effect. *Physical Review B*, 50(23):17199–17207, December 1994.
- [53] Alexander Seidel. Pfaffian Statistics through Adiabatic Transport in the 1D Coherent State Representation. *Physical Review Letters*, 101(19):196802, November 2008.
- [54] Alexander Seidel. S-duality constraints on 1D patterns associated with fractional quantum hall states. *Physical Review Letters*, 105(2):026802, July 2010.
- [55] Alexander Seidel, Henry Fu, Dung-Hai Lee, Jon Magne Leinaas, and Joel Moore. Incompressible quantum liquids and new conservation laws. *Physical Review Letters*, 95(26):266405, December 2005.
- [56] Alexander Seidel and Dung-Hai Lee. Abelian and non-abelian hall liquids and charge-density wave: Quantum number fractionalization in one and two dimensions. *Physical Review Letters*, 97:056804, Aug 2006.
- [57] Alexander Seidel and Dung-Hai Lee. Domain-wall-type defects as anyons in phase space. *Phys. Rev. B*, 76:155101, Oct 2007.
- [58] Alexander Seidel and Kun Yang. Gapless excitations in the haldane-rezayi state: The thin-torus limit. *Physical Review B*, 84(8):085122, August 2011.

- [59] Steven H. Simon, E. H. Rezayi, N. R. Cooper, and I. Berdnikov. Construction of a paired wave function for spinless electrons at filling fraction $\nu = 25$. *Physical Review B*, 75:075317, Feb 2007.
- [60] Zlatko Tešanović. Charge modulation, spin response, and dual hofstadter butterfly in high- T_c cuprates. *Phys. Rev. Lett.*, 93:217004, Nov 2004.
- [61] D. J. Thouless, M. Kohmoto, M. P. Nightingale, and M. den Nijs. Quantized hall conductance in a two-dimensional periodic potential. *Phys. Rev. Lett.*, 49:405–408, Aug 1982.
- [62] S. A. Trugman and S. Kivelson. Exact results for the fractional quantum hall effect with general interactions. *Physical Review B*, 31:5280–5284, Apr 1985.
- [63] D. C. Tsui, H. L. Stormer, and A. C. Gossard. Two-dimensional magnetotransport in the extreme quantum limit. *Physical Review Letters*, 48(22):1559–1562, May 1982.
- [64] O. Vafek, A. Melikyan, M. Franz, and Z. Tešanović. Quasiparticles and vortices in unconventional superconductors. *Phys. Rev. B*, 63(13):134509, March 2001.
- [65] O. Vafek, A. Melikyan, and Z. Tešanović. Quasiparticle hall transport of d-wave superconductors in the vortex state. *Phys. Rev. B*, 64(22):224508, November 2001.
- [66] Oskar Vafek. Anomalous scaling and gapless fermions of d-Wave superconductors in a magnetic field. *Phys. Rev. Lett.*, 99(4):047002, July 2007.
- [67] Oskar Vafek and Ashot Melikyan. Index theoretic characterization of d-Wave superconductors in the vortex state. *Phys. Rev. Lett.*, 96(16):167005, April 2006.
- [68] Ashvin Vishwanath. Quantized thermal hall effect in the mixed state of d -wave superconductors. *Phys. Rev. Lett.*, 87:217004, Nov 2001.
- [69] Ashvin Vishwanath. Dirac nodes and quantized thermal hall effect in the mixed state of d -wave superconductors. *Phys. Rev. B*, 66:064504, Aug 2002.
- [70] Hao Wang and V. W. Scarola. Jastrow-correlated wave functions for flat-band lattices. *Physical Review B*, 83(24):245109, June 2011.
- [71] Yong Wang and A. H. MacDonald. Mixed-state quasiparticle spectrum for d-wave superconductors. *Phys. Rev. B*, 52(6):R3876, 1995.
- [72] X. G. Wen and Q. Niu. Ground-state degeneracy of the fractional quantum hall states in the presence of a random potential and on high-genus riemann surfaces. *Physical Review B*, 41(13):9377–9396, May 1990.
- [73] John A. Wheeler. *Geometrodynamics*. Acad. Press, 1962.
- [74] R. Willett, J. P. Eisenstein, H. L. Stormer, D. C. Tsui, A. C. Gossard, and J. H. English. Observation of an even-denominator quantum number in the fractional quantum hall effect. *Physical Review Letters*, 59(15):1776–1779, October 1987.

- [75] Daijiro Yoshioka. Excitation energies of the fractional quantum hall effect. *Journal of the Physical Society of Japan*, 55(3):885–896, 1986.
- [76] Daijiro Yoshioka. *The Quantum Hall Effect*. Springer, April 2002.
- [77] Zhenyu Zhou, Zohar Nussinov, and Alexander Seidel. Heat equation approach to geometric changes of the torus Laughlin state. *Physical Review B*, 87(11):115103, March 2013.
- [78] Zhenyu Zhou, Oskar Vafek, and Alexander Seidel. Geometric phases of d-wave vortices in a model of lattice fermions. *Physical Review B*, 86(2):020505, July 2012.